

Appendix E

Polarity problems at selected stations in southern California

Note

I am fortunate to have had close contact with the Southern California Data Center. I thank Ellen Yu, Egill Hauksson, and Kate Hutton for discussions regarding the matters presented in this appendix. The key results are summarized in Table E.1.

E.1 Overview

Our tomography study for southern California has aimed to incorporate three-component waveform data from all available broadband stations for 234 earthquakes, $M_w = 3.5\text{--}5.5$, over the time period 1998–2009. For these earthquakes we have generated synthetic seismograms using a 3D crustal model provided by the Southern California Earthquake Center, which we improved with 16 iterations in a tomographic inversion. Based on thousands of comparisons between synthetic and recorded seismograms, I have discovered a problem with the polarity of certain stations for specific epochs. The polarity problem is summarized in Table E.1 and in the following figures. I demonstrate the problematic records using the seismograms filtered at relatively long periods (bandpass 6–30 s), which are not as sensitive to possible “site effect,” i.e., strong heterogeneity in the immediate region of the station. Because the station coverage in southern California is dense, it is usually possible to find a nearby station to the problematic one, in order to demonstrate the problem. One example

Table E.1: Southern California station–epochs with problematic polarity. “Earthquake dates” indicates the earliest and latest earthquakes within my dataset that exhibit the identified polarity problem on records bandpassed 6–30 s. These dates were used to identify the problematic epochs for each station.

Station	Earthquake dates		Corresponding Epochs		Channels (BH _L)	Figures
	Earliest	Latest	Start	End		
CRP.CI	2003–12–25	2006–06–30	2003.297 2003.301 2006.114	2003.301 2006.114 2006.212	Z, E, N	E.1
HWB.AZ	2003–05–24	2008–07–29	2003.099 2004.056	2004.056 99999	Z, E, N	E.3–E.4
BVDA2.AZ	2003–05–24	2007–02–09	2003.133 2004.056	2004.056 99999	Z, E, N	E.5–E.6
PER.CI	2003–12–04	2009–01–31	2003.141 2003.147 2006.157 2008.305	2003.147 2006.157 2008.305 99999	E, N	E.7–E.9
BTP.CI	2002–10–29	2003–03–11	2002.297	2003.071	E, N	E.10–E.12
NSS2.CI	2004–09–29	2005–09–02	2004.077	2006.125	E, N	E.13–E.15
109C.TA	2004–07–14	2005–10–18	2004.125 2005.101	2005.101 2007.242	E, N	E.16–E.18
OSI.CI	1998-01-05	1998-10-27	1995.179(?)	2002.196(?)	E(?)	E.19–E.22

is shown in Figures E.7–E.9 for station PER.CI for an earthquake on 2008.12.06. From stations MSJ.CI to PER.CI to RVR.CI, I sweep the azimuth in a clockwise manner. The records for MSJ and RVR are similar, but the station in between, BTP, has the polarity flipped for both the transverse (T) and radial (R) components.

Most of the stations with reported polarity problems are not exhibiting the problems at present. In other words, the problems are restricted to specific epochs of the stations, and may be restricted to particular components as well (Table E.1). Of course, it is most important that the stations are providing accurate waveforms at present time, in order to properly record future earthquakes. However, it is also important that the waveforms in the past are accurate as well, since these waveforms may be used to improve the current 3D structure model or to simulate past earthquakes. In most of the cases presented below, it would be a relatively simple matter of adjusting the sign within the station response files (i.e., dataless seed files), and then the waveforms would be usable.

I also observed a problem with station amplifications for three stations recording events prior to 2000 (Section E.3). Detecting systematic amplifications is more subtle than detecting the polarity problems. An example of the amplification is shown in Figures E.23–E.25: the relative-low amplitude on all three components at VCS (Figure E.24) is not observed at stations in azimuthal directions on either side of VCS (Figures E.23 and E.25).

E.2 Station–epochs with probable incorrect polarity (Figures E.1–E.22)

- CRP.CI: Figure E.1. From the 3D synthetics, it appears that the seismograms (all three components) are “good”, but flipped upsidedown. In Figure E.2, I show the effect of simply flipping the sign of `CONSTANT` in the pole-zero file. A sign flip appears to solve the problem for this station. NOTE: CRP.CI is fine as of 2006.11.03 (10215753).
- HWB.AZ: Figures E.3–E.4. From the 3D synthetics, it appears that the seismograms (all three components) are “good”, only flipped upsidedown.

There is something peculiar about HWB.AZ records. By 2008.12.06 (14408052), HWB.AZ records look great, but the PZ file is the same as before. This suggests that HWB.AZ was changed, but the dataless seed file was not updated.

- BVDA2.AZ: Figures E.5–E.6. From the 3D synthetics, it appears that the seismograms (all three components) are “good”, only flipped upsidedown.
- PER.CI: Figures E.7–E.9. From stations MSJ.CI to PER.CI to RVR.CI, I sweep the azimuth in a clockwise manner. The records for MSJ and RVR are similar, but the station in between, BTP, has the polarity flipped for both the transverse (T) and radial (R) components. The earthquake occurred near Hector Mine on 2008.12.06.
- BTP.CI: Figures E.10–E.12. From stations ALP.CI to BTP.CI to OSI.CI, I sweep the azimuth in a clockwise manner. The records for ALP and OSI are similar, but the station in between, BTP, has the polarity flipped for both the transverse (T) and radial (R) components.
- NSS2.CI: Figures E.13–E.15. From stations CTC.CI to NSS2.CI to THX.CI, I sweep the azimuth in a clockwise manner. The records for CTC and THX are similar, but the station in between, NSS2, has the polarity flipped for both the transverse (T) and radial (R) components.
- 109C.TA: Figures E.16–E.18. From stations SDR.CI to 109C.TA to SDG.CI, I sweep the azimuth in a clockwise manner. It appears that something is wrong with the horizontal components for 109C.TA, though it may not be a simply sign error or switch between the E and N components.
- OSI.CI. Figures E.19 and E.22. The pattern for OSI.CI suggests that only the east component has a polarity problem, or that there was some misalignment of the horizontal components. For earthquakes from an easterly direction, the problem is more apparent on the radial component (Figures E.19 and E.20). For earthquakes from a northerly direction, the problem is more apparent on the transverse component (Figures E.21 and E.22).

There is something peculiar about the 1998 OSI.CI records. All of the problematic records occur in 1998, but the PZ file indicates the same epoch through 2002. This suggests that OSI.CI was changed, but the dataless seed file was not updated. Also, even *between* the earliest (1998-01-05) and latest (1998-10-27) identified problematic records, there are some *good* records: 9064093 (1998-08-16) and 9065468 (1998-08-20).

Detailed list of seismograms exhibiting polarity problems

Figures E.1 and E.2 show one example for one station (CRP.CI). I will now list all the paths for which the polarity on **all three components** appears to be flipped:

1. **CRP.CI.** 9968977 9983429 10059745 10097009 10100053 10148421 14073800 14077668
14095540 14095628 14096196 14116972 14138080 14151344 14155260 14165408 14169456
14178236 14178248 14186612 14236768
2. **HWB.AZ.** 9967901 10100053 10215753 13966396 14095628 14096196 14151344 14155260
14178184 14178188 14178212 14178236 14178248 14179292 14179736 14236768 14263712
14263716 14383980
3. **BVDA2.AZ.** 9967901 10215753 10230869 13966396 14095540 14095628 14169456
14178184 14178188 14178212 14178236 14178248 14179288 14179292 14179736 14186612
14233632 14236768 14263544 14263712 14263716

Figures E.7–E.9 shows one example for one station (PER.CI). I will now list all the paths for which the polarity on the **horizontal components only** appears to be a problem:

1. **BTP.CI.** 9854597 9882325 9882329 13935988 13936812 13938812 13945908
2. **PER.CI.** 9967901 9968977 9983429 10006857 10059745 10063349 10097009 10100053
10148421 10215753 10230869 10370141 14007388 14072464 14073800 14077668 14095540
14095628 14096196 14116972 14118096 14133048 14138080 14151344 14158696 14169456
14178184 14178188 14178212 14178236 14178248 14179288 14179292 14179736 14186612
14236768 14239184 14263544 14383980 14408052 10370141 14418600
3. **NSS2.CI.** 10059745 10097009 14095628 14138080 14151344 14155260 14178184 14178188
14178248 14179292 14179736
4. **109C.TA.** 10059745 10097009 10100053 10148421 14073800 14095628 14116972 14118096
14138080 14151344 14155260 14169456 14178184 14178188 14178212 14178236 14178248
14179288 14179292 14179736 14186612
5. **OSI.CI (BHE only?).** 3298292 (BHR) 9038699 (BHR) 9069997 (BHR) 9044650
(BHT) 9045109 (BHT) 9045697 (BHT)

Next I list all the events above in order of increasing origin time, with each problematic station listed on the following line(s). Note that these records are only the ones that I have identified directly as having a problem. I expect that records at the same stations during the same epochs would exhibit the **polarity problem** as well.

9038699	1998-01-05	18:14:06	Mw 3.9	-117.7178	33.9462	12.98 km
	OSI.CI-E					
9044650	1998-03-06	07:36:35	Mw 4.0	-117.6505	36.0737	7.93 km
	OSI.CI-E					
9045109	1998-03-07	00:36:46	Mw 4.5	-117.6200	36.0912	6.99 km
	OSI.CI-E					
9045697	1998-03-08	15:28:41	Mw 3.7	-117.6133	36.0827	4.81 km
	OSI.CI-E					
3298292	1998-03-11	12:18:51	Mw 4.2	-117.2222	34.0355	16.19 km
	OSI.CI-E					
9069997	1998-10-27	01:08:40	Mw 4.4	-116.8418	34.3208	6.02 km
	OSI.CI-E					
9854597	2002-10-29	14:16:54	Mw 4.4	-116.2650	34.8068	7.89 km
	BTP.CI-EN					
9882325	2003-01-25	09:11:02	Mw 3.9	-118.6632	35.3152	4.41 km
	BTP.CI-EN					
9882329	2003-01-25	09:16:10	Mw 4.2	-118.6585	35.3128	4.12 km
	BTP.CI-EN					
13935988	2003-02-22	12:19:10	Mw 4.8	-116.8460	34.3103	4.55 km
	BTP.CI-EN					
13936812	2003-02-22	19:33:45	Mw 4.2	-116.8482	34.3097	4.87 km
	BTP.CI-EN					
13938812	2003-02-25	04:03:04	Mw 4.0	-116.8407	34.3137	3.84 km
	BTP.CI-EN					
13945908	2003-03-11	19:28:17	Mw 4.2	-116.1303	34.3582	8.08 km
	BTP.CI-EN					
13966396	2003-05-24	02:04:28	Mw 4.1	-115.5538	32.9475	8.72 km
	HWB.AZ-ZEN					
	BVDA2.AZ-ZEN					
14007388	2003-12-04	06:15:52	Mw 3.5	-117.5664	35.6352	2.13 km
	PER.CI-EN					
9967901	2003-12-23	18:17:11	Mw 4.5	-121.0428	35.6493	7.20 km
	PER.CI-EN					
	HWB.AZ-ZEN					
	BVDA2.AZ-ZEN					
9968977	2003-12-25	11:50:01	Mw 4.3	-120.8385	35.5487	8.18 km
	PER.CI-EN					
	CRP.CI-ZEN					
9983429	2004-02-14	12:43:11	Mw 4.5	-119.1412	35.0118	11.81 km
	PER.CI-EN					
	CRP.CI-ZEN					
10006857	2004-05-09	08:57:17	Mw 4.2	-120.0142	34.4135	10.97 km
	PER.CI-EN					
14072464	2004-07-09	04:43:45	Mw 3.7	-115.7441	32.5392	10.37 km
	PER.CI-EN					
14073800	2004-07-14	00:53:52	Mw 3.8	-116.0520	33.7152	12.20 km
	PER.CI-EN					
	109C.TA-EN					
	CRP.CI-ZEN					
14077668	2004-07-24	12:55:19	Mw 4.0	-119.4365	34.3885	8.66 km
	PER.CI-EN					
	CRP.CI-ZEN					
14095540	2004-09-29	17:10:04	Mw 4.8	-120.5134	35.9528	10.69 km
	PER.CI-EN					
	CRP.CI-ZEN					
	BVDA2.AZ-ZEN					
14095628	2004-09-29	22:54:54	Mw 4.8	-118.6292	35.3852	7.66 km
	NSS2.CI-EN					
	PER.CI-EN					
	109C.TA-EN					
	CRP.CI-ZEN					
	HWB.AZ-ZEN					
	BVDA2.AZ-ZEN					
14096196	2004-09-30	18:54:29	Mw 4.6	-120.5403	35.9821	9.87 km
	PER.CI-EN					
	CRP.CI-ZEN					
	HWB.AZ-ZEN					
10059745	2004-11-13	17:39:16	Mw 3.8	-116.8413	34.3533	10.31 km
	NSS2.CI-EN					
	PER.CI-EN					
	109C.TA-EN					
	CRP.CI-ZEN					
10063349	2004-11-29	01:54:14	Mw 4.0	-120.4963	35.9437	10.19 km
	PER.CI-EN					
14116972	2005-01-06	14:35:27	Mw 4.1	-117.4438	34.1272	5.04 km
	PER.CI-EN					
	109C.TA-EN					
	CRP.CI-ZEN					
14118096	2005-01-12	08:10:46	Mw 3.9	-116.3912	33.9578	8.51 km
	PER.CI-EN					
	109C.TA-EN					

14133048	2005-03-22	08:55:05	Mw 3.6	-116.2515	33.2884	4.74 km
	PER. CI-EN					
14138080	2005-04-16	19:18:13	Mw 4.6	-119.1940	34.9987	10.16 km
	NSS2. CI-EN					
	PER. CI-EN					
	109C. TA-EN					
	CRP. CI-ZEN					
10097009	2005-05-06	02:29:09	Mw 4.0	-119.1958	35.0023	13.01 km
	NSS2. CI-EN					
	PER. CI-EN					
	109C. TA-EN					
	CRP. CI-ZEN					
10100053	2005-05-16	07:24:37	Mw 4.2	-120.4792	35.9269	9.15 km
	PER. CI-EN					
	109C. TA-EN					
	CRP. CI-ZEN					
	HWB. AZ-ZEN					
14151344	2005-06-12	15:41:46	Mw 5.1	-116.5675	33.5380	13.91 km
	NSS2. CI-EN					
	PER. CI-EN					
	109C. TA-EN					
	CRP. CI-ZEN					
	HWB. AZ-ZEN					
14155260	2005-06-16	20:53:25	Mw 4.8	-117.0072	34.0612	14.19 km
	NSS2. CI-EN					
	109C. TA-EN					
	CRP. CI-ZEN					
	HWB. AZ-ZEN					
14158696	2005-06-27	22:17:33	Mw 3.6	-117.0232	34.0615	13.63 km
	PER. CI-EN					
14165408	2005-07-24	12:59:42	Mw 3.8	-119.7527	33.6853	3.85 km
	CRP. CI-ZEN					
14169456	2005-08-06	05:40:33	Mw 3.9	-118.0652	36.1488	3.67 km
	PER. CI-EN					
	109C. TA-EN					
	CRP. CI-ZEN					
	BVDA2. AZ-ZEN					
14178184	2005-08-31	22:47:45	Mw 4.7	-115.6207	33.1544	4.50 km
	NSS2. CI-EN					
	PER. CI-EN					
	109C. TA-EN					
	HWB. AZ-ZEN					
	BVDA2. AZ-ZEN					
14178188	2005-08-31	22:50:24	Mw 4.4	-115.6098	33.1639	1.59 km
	NSS2. CI-EN					
	PER. CI-EN					
	109C. TA-EN					
	HWB. AZ-ZEN					
	BVDA2. AZ-ZEN					
14178212	2005-08-31	23:07:16	Mw 4.3	-115.6157	33.1548	5.01 km
	PER. CI-EN					
	109C. TA-EN					
	HWB. AZ-ZEN					
	BVDA2. AZ-ZEN					
14178236	2005-08-31	23:27:32	Mw 4.1	-115.5924	33.1748	3.95 km
	PER. CI-EN					
	109C. TA-EN					
	CRP. CI-ZEN					
	HWB. AZ-ZEN					
	BVDA2. AZ-ZEN					
14178248	2005-08-31	23:32:11	Mw 4.3	-115.5969	33.1712	5.05 km
	NSS2. CI-EN					
	PER. CI-EN					
	109C. TA-EN					
	CRP. CI-ZEN					
	HWB. AZ-ZEN					
	BVDA2. AZ-ZEN					
14179288	2005-09-01	13:48:25	Mw 3.8	-115.6168	33.1538	4.74 km
	PER. CI-EN					
	109C. TA-EN					
	BVDA2. AZ-ZEN					
14179292	2005-09-01	13:50:20	Mw 4.4	-115.6064	33.1643	2.63 km
	NSS2. CI-EN					
	PER. CI-EN					
	109C. TA-EN					
	HWB. AZ-ZEN					
	BVDA2. AZ-ZEN					
14179736	2005-09-02	01:27:20	Mw 5.0	-115.6295	33.1479	4.90 km
	NSS2. CI-EN					
	PER. CI-EN					
	109C. TA-EN					
	HWB. AZ-ZEN					
	BVDA2. AZ-ZEN					
14186612	2005-09-22	20:24:48	Mw 4.4	-119.0247	35.0178	10.24 km
	PER. CI-EN					
	109C. TA-EN					
	CRP. CI-ZEN					
	BVDA2. AZ-ZEN					
10148421	2005-10-18	07:31:03	Mw 4.1	-116.7715	34.0182	18.32 km
	PER. CI-EN					
	109C. TA-EN					
	CRP. CI-ZEN					

14236768	2006-06-30	00:28:06	Mw 4.1	-116.0220	33.2450	3.84 km
	PER.CI-EN					
	CRP.CI-ZEN					
	HWB.AZ-ZEN					
	BVDA2.AZ-ZEN					
14239184	2006-07-10	02:54:43	Mw 3.7	-117.1103	33.8567	16.77 km
	PER.CI-EN					
10215753	2006-11-03	15:56:43	Mw 4.1	-116.0520	32.7165	14.76 km
	PER.CI-EN					
	HWB.AZ-ZEN					
	BVDA2.AZ-ZEN					
14263544	2006-11-29	12:17:35	Mw 3.7	-115.9628	32.8423	3.37 km
	PER.CI-EN					
	BVDA2.AZ-ZEN					
14263712	2006-11-29	21:10:55	Mw 4.0	-115.9672	32.8385	7.16 km
	HWB.AZ-ZEN					
	BVDA2.AZ-ZEN					
14263716	2006-11-29	21:12:52	Mw 3.6	-115.9672	32.8377	3.43 km
	HWB.AZ-ZEN					
	BVDA2.AZ-ZEN					
10230869	2007-02-09	03:33:43	Mw 3.9	-116.1357	33.2220	20.99 km
	PER.CI-EN					
	BVDA2.AZ-ZEN					
14383980	2008-07-29	18:42:16	Mw 5.4	-117.7610	33.9530	14.23 km
	PER.CI-EN					
	HWB.AZ-ZEN					
14408052	2008-12-06	04:18:43	Mw 5.0	-116.4190	34.8130	6.10 km
	PER.CI-EN					
10370141	2009-01-09	03:49:46	Mw 4.4	-117.3040	34.1070	14.20 km
	PER.CI-EN					
14418600	2009-01-31	21:09:22	Mw 3.9	-117.7860	35.4130	8.50 km
	PER.CI-EN					

E.3 Station–epochs with probable incorrect amplification (Figures E.23–E.29)

- VCS.CI: Figures E.23–E.25. The relative-low amplitude on all three components at VCS (Figure E.24) is not observed at stations in azimuthal directions on either side of VCS (Figures E.23 and E.25).
- SMTC.AZ: Figures E.26 and E.27. The relative-low amplitude for BHZ and BHT at SMTC.AZ (Figure E.24) is not observed at adjacent station SWS.CI (Figure E.26).
- BAR.CI: Figures E.28 and E.29. It is possible that for BAR.CI the amplification problem is only with the east component. This inference is based on the fact that the amplification is observed primarily on the transverse component for north-south paths (Figures E.28 and E.29), and it is observed primarily on the radial component for east-west paths (9075803, 9154092).

Detailed list of seismograms exhibiting amplification problems

- VCS.CI: 7112721 9044494 9044650 9045109 9064093 9064568 9069997 9070083
- SMTC.AZ: 3317364 9075803 9086693

- BAR.CI: 9075803 (R) 9154092 (R) 3320736 (T) 3321426 (T) 3321590 (T) 9085734 (T) 9109287 (T) 9109442 (T) 9109636 (T) 9110685 (T) 9112735 (T) 9114763 (T) 9114812 (T) 9114858 (T) 9117942 (T) 9119414 (T) 9140050 (T)

Next I list all the events above in order of increasing origin time, with each problematic station listed on the following line(s). Note that these records are only the ones that I have identified directly as having a problem. I expect that records at the same stations during the same epochs would exhibit the **amplification problem** as well.

9044494	1998-03-06	05:47:40	Mw 4.9	-117.6405	36.0778	7.17 km
VCS.CI-ZEN						
9044650	1998-03-06	07:36:35	Mw 4.0	-117.6505	36.0737	7.93 km
VCS.CI-ZEN						
9045109	1998-03-07	00:36:46	Mw 4.5	-117.6200	36.0912	6.99 km
VCS.CI-ZEN						
9064093	1998-08-16	13:34:40	Mw 4.4	-116.9232	34.1245	5.98 km
VCS.CI-ZEN						
9064568	1998-08-20	23:49:58	Mw 4.1	-117.6502	34.3737	9.51 km
VCS.CI-ZEN						
7112721	1998-10-01	18:18:15	Mw 4.2	-116.9158	34.1155	5.40 km
VCS.CI-ZEN						
9069997	1998-10-27	01:08:40	Mw 4.4	-116.8418	34.3208	6.02 km
VCS.CI-ZEN						
9070083	1998-10-27	15:40:16	Mw 3.8	-116.8455	34.3202	5.48 km
VCS.CI-ZEN						
9075803	1999-01-13	13:20:56	Mw 4.2	-115.9248	32.7190	8.00 km
SMT.AZ-ZEN						
BAR.CI-E						
9085734	1999-05-05	02:17:46	Mw 3.6	-116.3697	34.0725	2.58 km
BAR.CI-E						
9086693	1999-05-14	08:22:07	Mw 3.9	-116.3623	34.0375	3.98 km
SMT.AZ-ZEN						
3317364	1999-05-14	10:52:35	Mw 4.1	-116.3582	34.0378	4.01 km
SMT.AZ-ZEN						
3320736	1999-10-16	12:57:21	Mw 5.3	-116.2465	34.4368	7.96 km
BAR.CI-E						
9109287	1999-10-16	18:01:57	Mw 4.0	-116.3013	34.7087	6.65 km
BAR.CI-E						
9109442	1999-10-16	20:13:37	Mw 4.3	-116.2793	34.6940	3.18 km
BAR.CI-E						
9109636	1999-10-16	22:53:41	Mw 4.1	-116.3570	34.7097	9.52 km
BAR.CI-E						
9110685	1999-10-17	16:22:48	Mw 4.1	-116.1375	34.3465	3.96 km
BAR.CI-E						
9112735	1999-10-19	12:20:44	Mw 4.0	-116.3442	34.7110	9.34 km
BAR.CI-E						
3321590	1999-10-21	01:54:34	Mw 4.8	-116.3955	34.8735	3.33 km
BAR.CI-E						
9114763	1999-10-22	12:40:52	Mw 3.7	-116.2085	34.3300	11.53 km
BAR.CI-E						
9114812	1999-10-22	16:08:48	Mw 4.8	-116.4060	34.8620	3.02 km
BAR.CI-E						
9114858	1999-10-22	16:48:22	Mw 3.8	-116.3820	34.8292	5.15 km
BAR.CI-E						
9117942	1999-10-29	12:36:37	Mw 4.0	-116.2707	34.5200	2.90 km
BAR.CI-E						
3321426	1999-11-03	02:55:05	Mw 3.6	-116.2888	34.8031	6.06 km
BAR.CI-E						
9119414	1999-11-03	03:27:57	Mw 3.9	-116.3570	34.8470	5.90 km
BAR.CI-E						
9140050	2000-02-21	13:49:43	Mw 4.1	-117.2432	34.0588	16.34 km
BAR.CI-E						
9154092	2000-06-14	19:00:20	Mw 4.3	-115.5035	32.8898	8.73 km
BAR.CI-E						

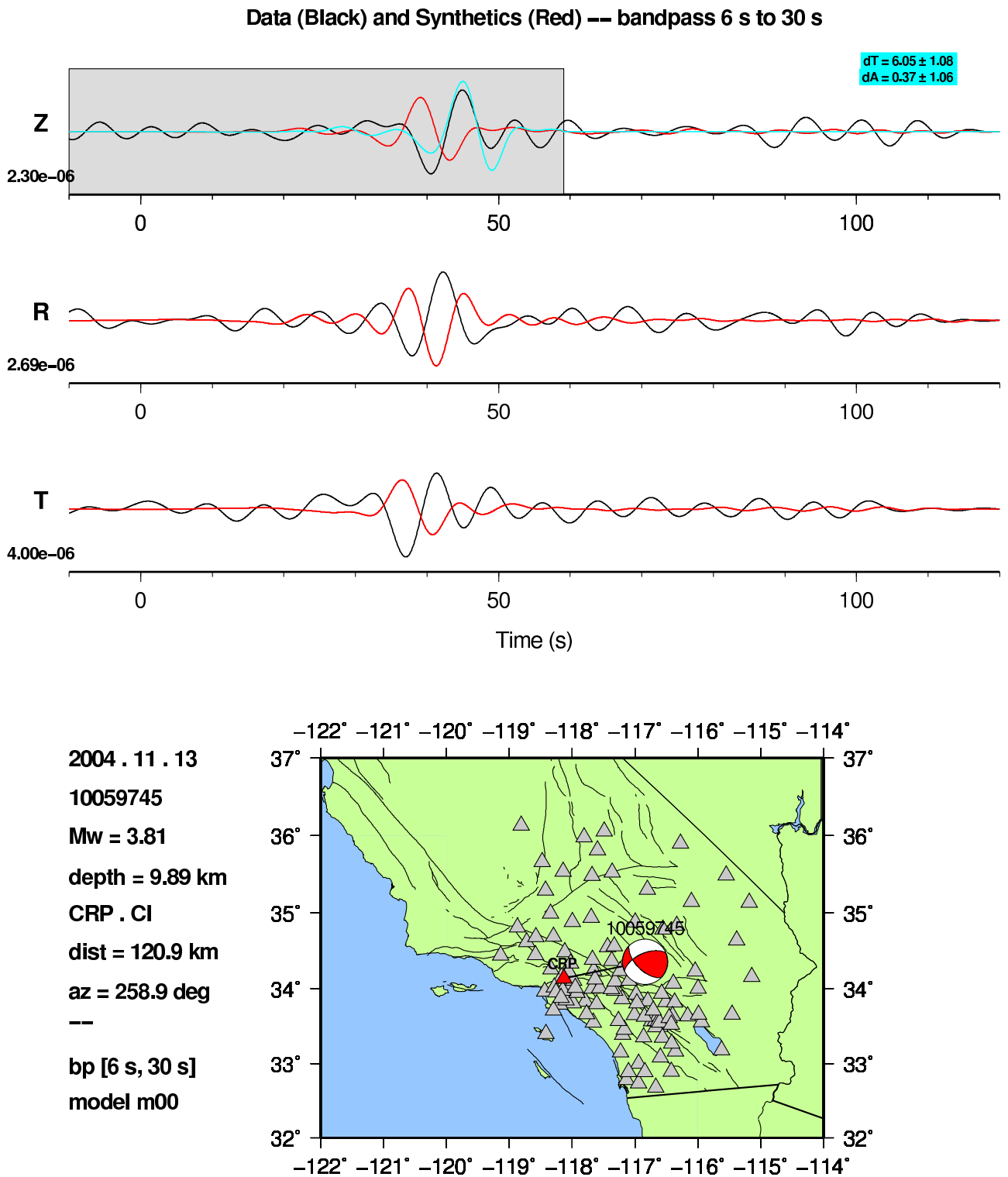
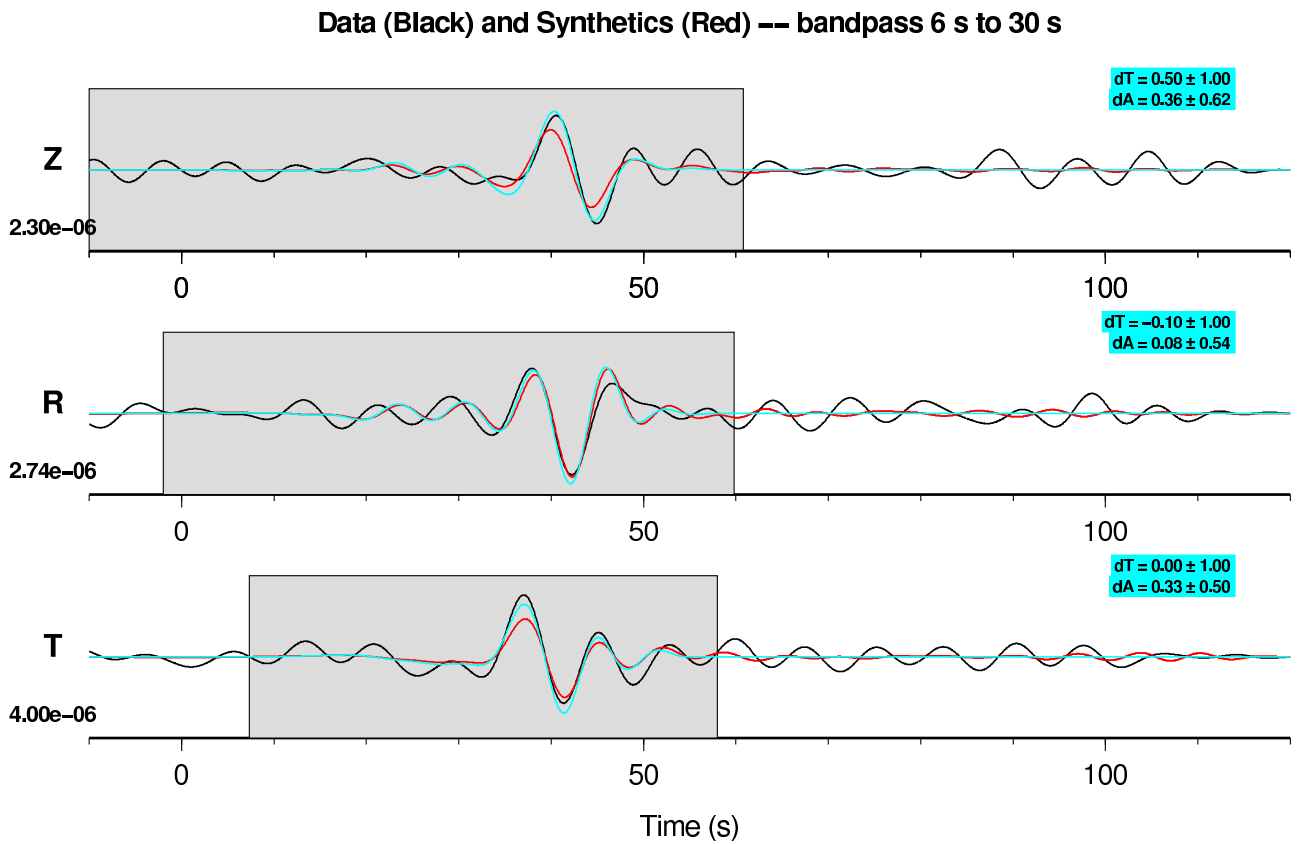


Figure E.1: Data (black) and synthetics (red), 6–30 s, from 10059745 to CRP.CI. The measurement algorithm selects a large time shift for the Rayleigh wave, but this is due to the station error, not to the source or structure. Compare with Figure E.2.



2004 . 11 . 13
10059745
Mw = 3.81
depth = 9.89 km
CRP . CI
dist = 120.9 km
az = 258.9 deg
--
bp [6 s, 30 s]
model m16

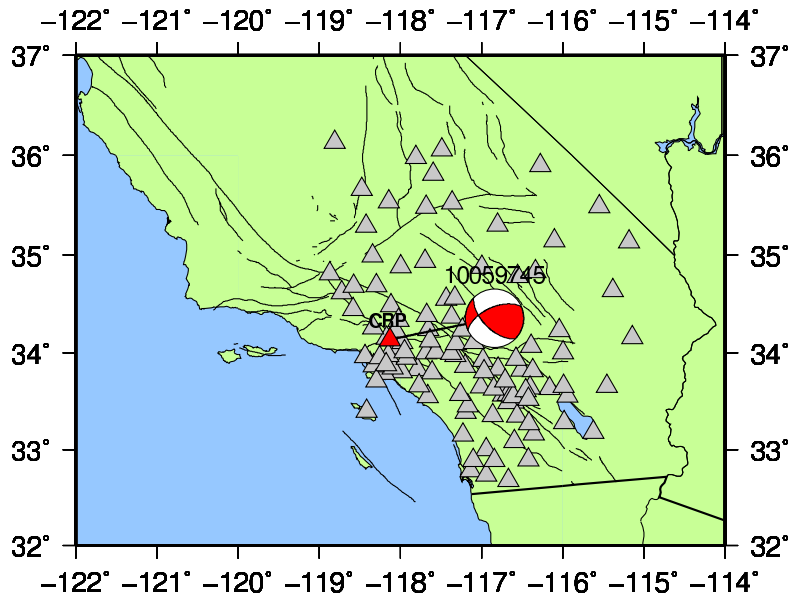
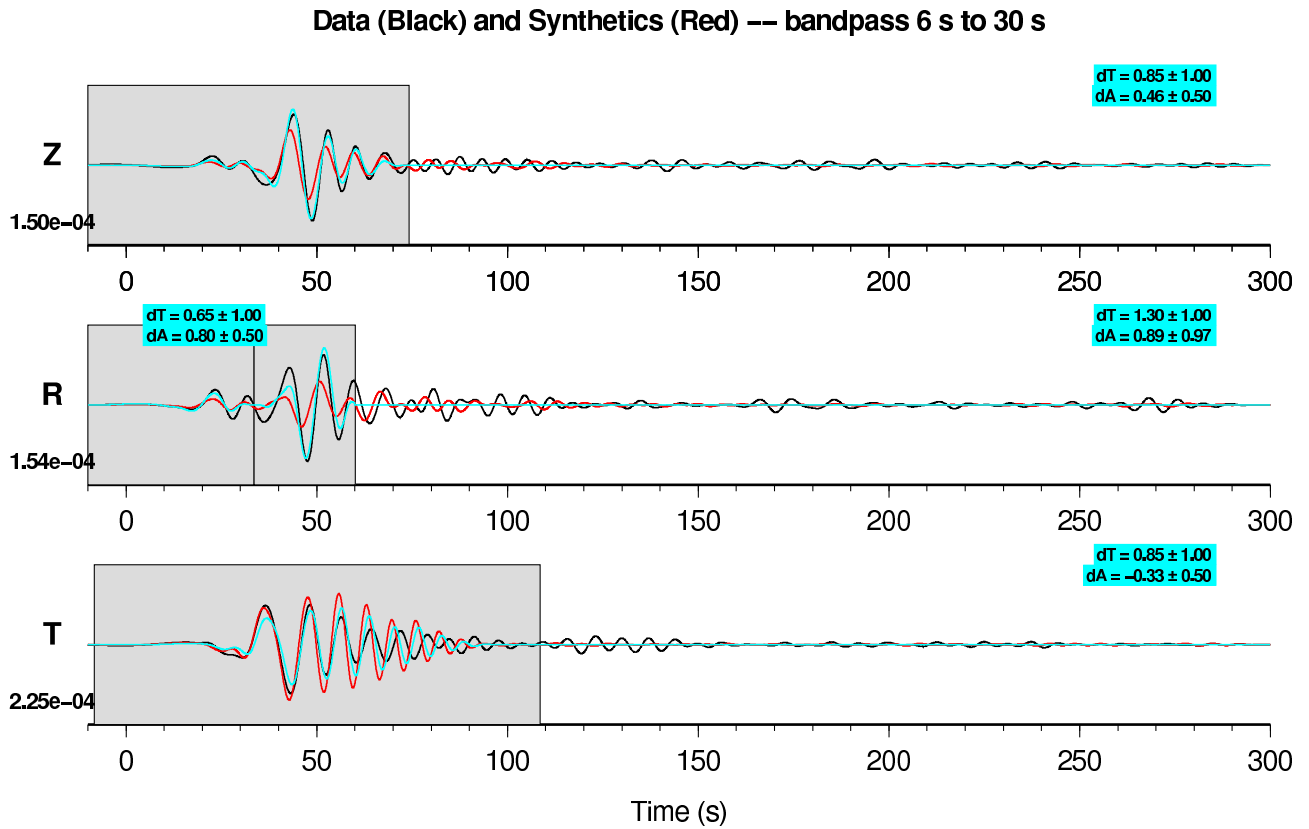


Figure E.2: Data (black) and synthetics (red), 6–30 s, from 10059745 to CRP.CI. In this case, I have flipped the sign of the constant value in the pole-zero file. Compare with Figure E.1.



2005 . 09 . 02
 14179736
 Mw = 4.97
 depth = 4.79 km
 DPP . CI
 dist = 123.6 km
 az = 262.7 deg
 --
 bp [6 s, 30 s]
 model m16

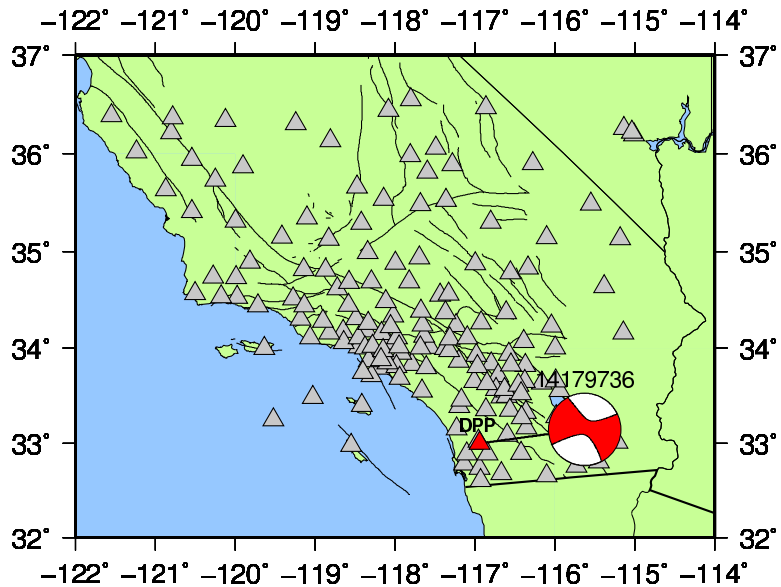


Figure E.3: Data (black) and synthetics (red), 6–30 s, from 14179736 to DPP.CI. Compare with Figure E.4.

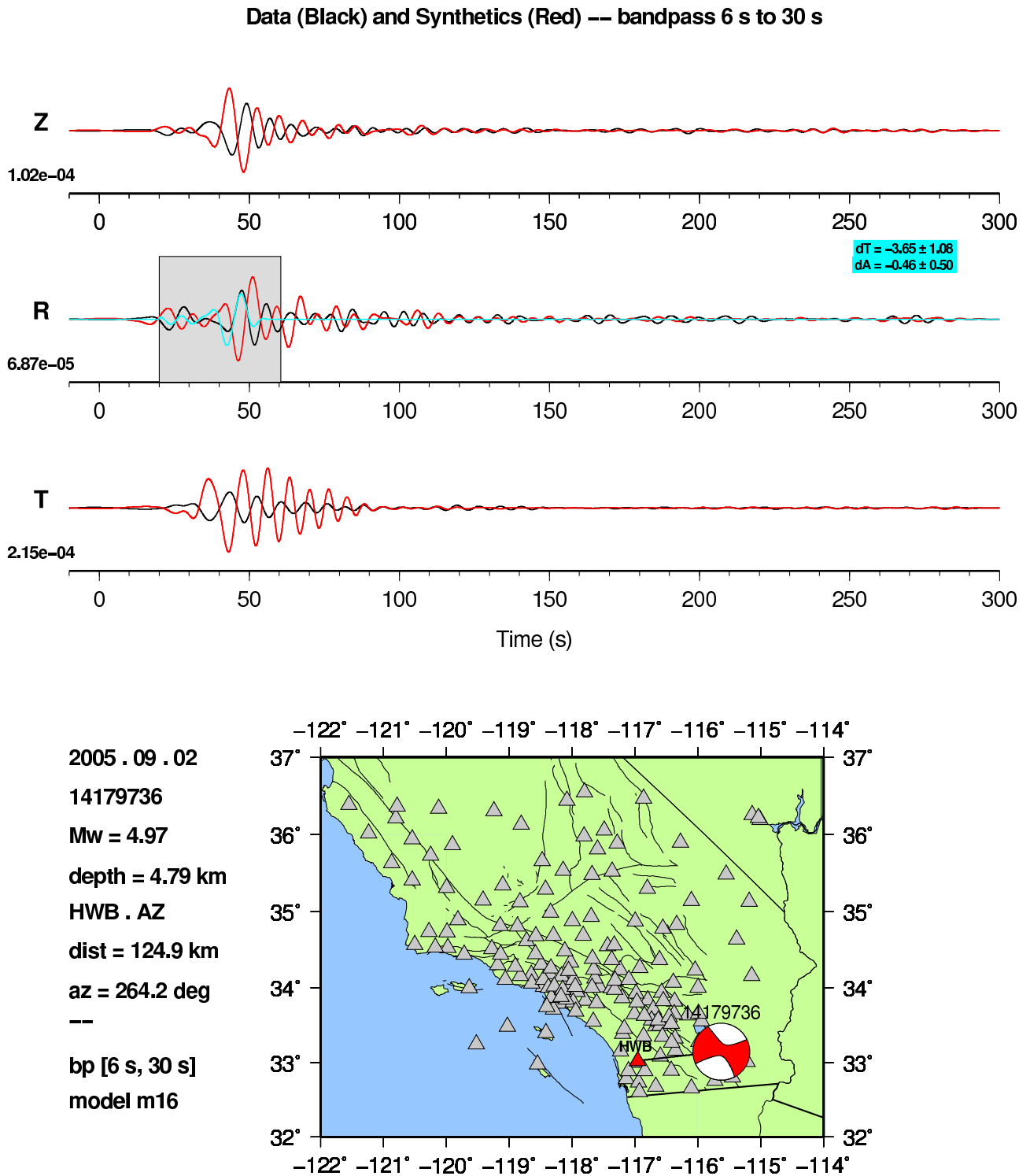
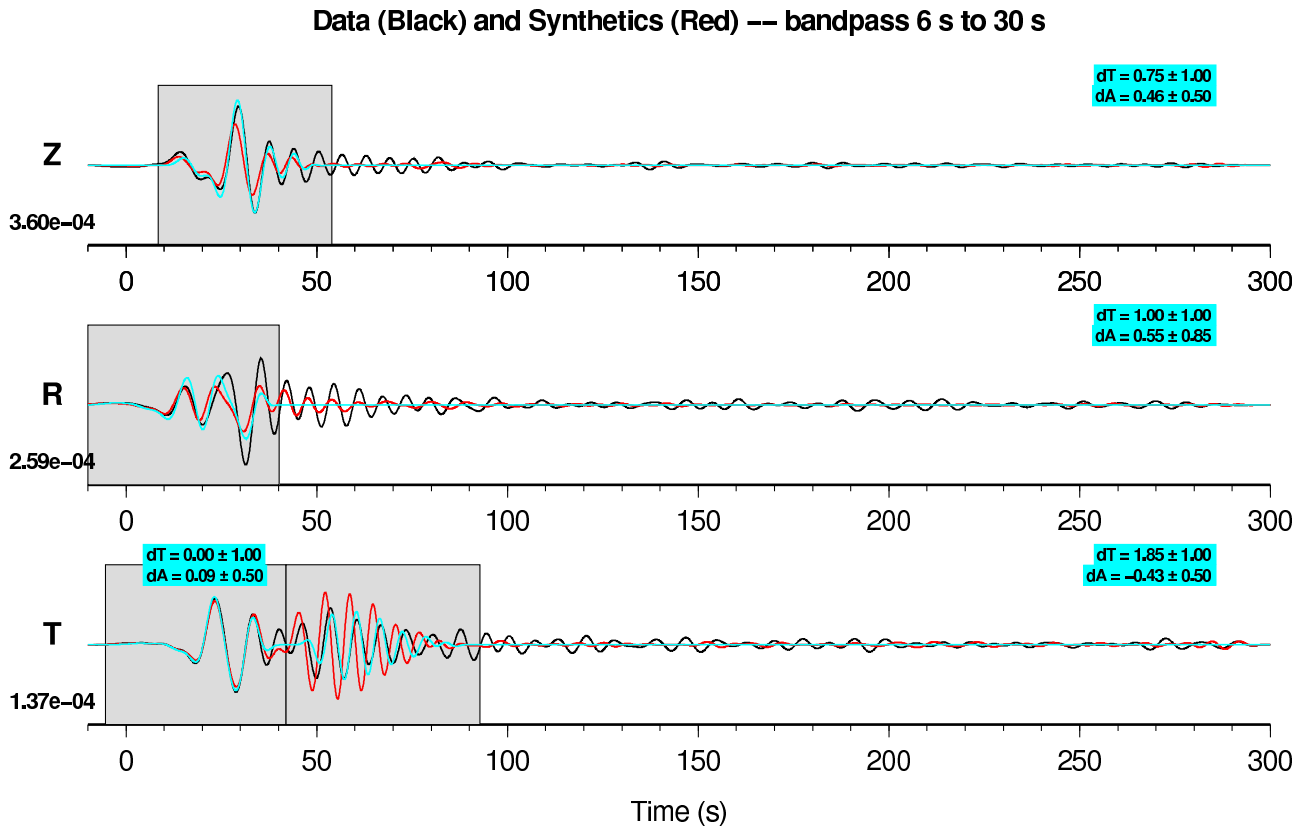


Figure E.4: Data (black) and synthetics (red), 6–30 s, from 14179736 to HWB.AZ. The measurement algorithm selects a large time shift for the radial-component Rayleigh wave, but this is due to the station error, not to the source or structure. Compare with Figure E.3.



2005 . 09 . 02
 14179736
 Mw = 4.97
 depth = 4.79 km
 BOR . CI
 dist = 74.6 km
 az = 280.5 deg
 --
 bp [6 s, 30 s]
 model m16

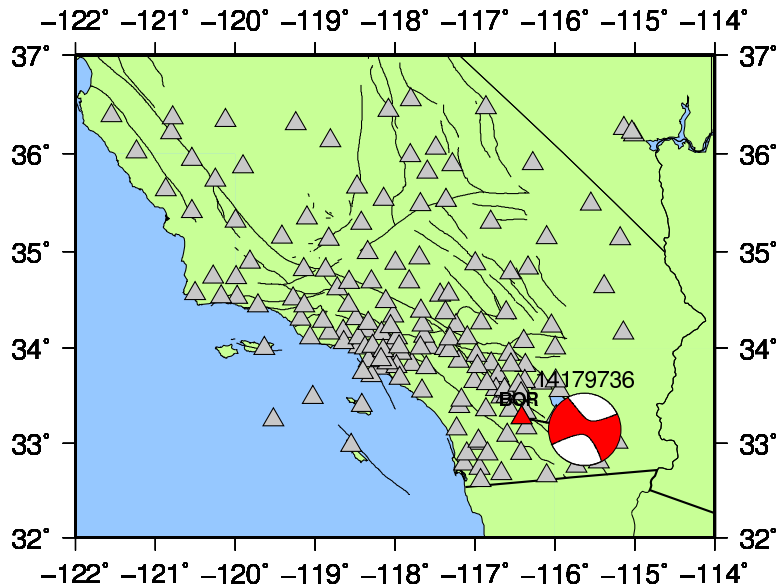


Figure E.5: Data (black) and synthetics (red), 6–30 s, from 14179736 to BOR.CI. Compare with Figure E.6.

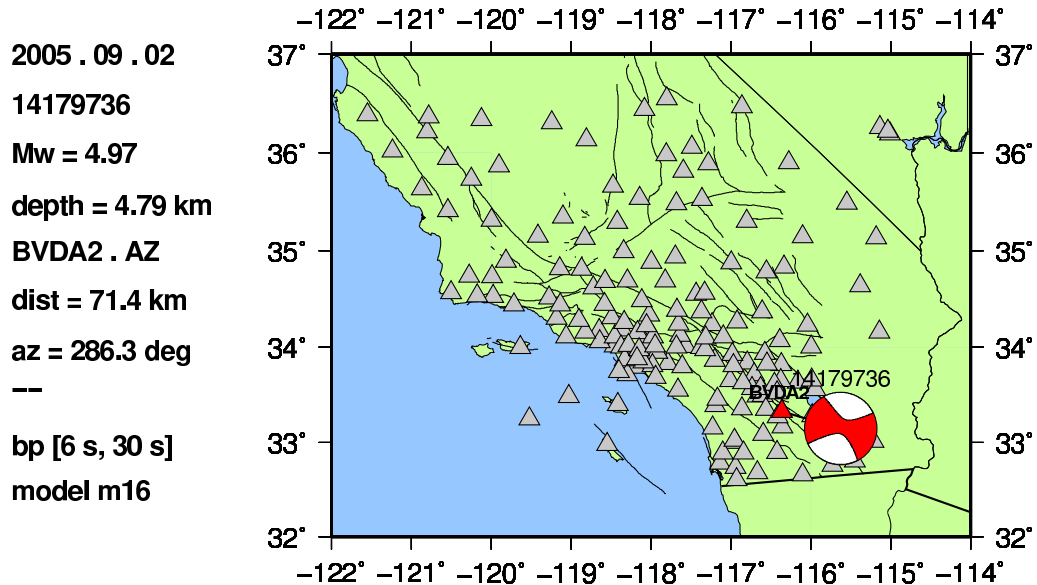
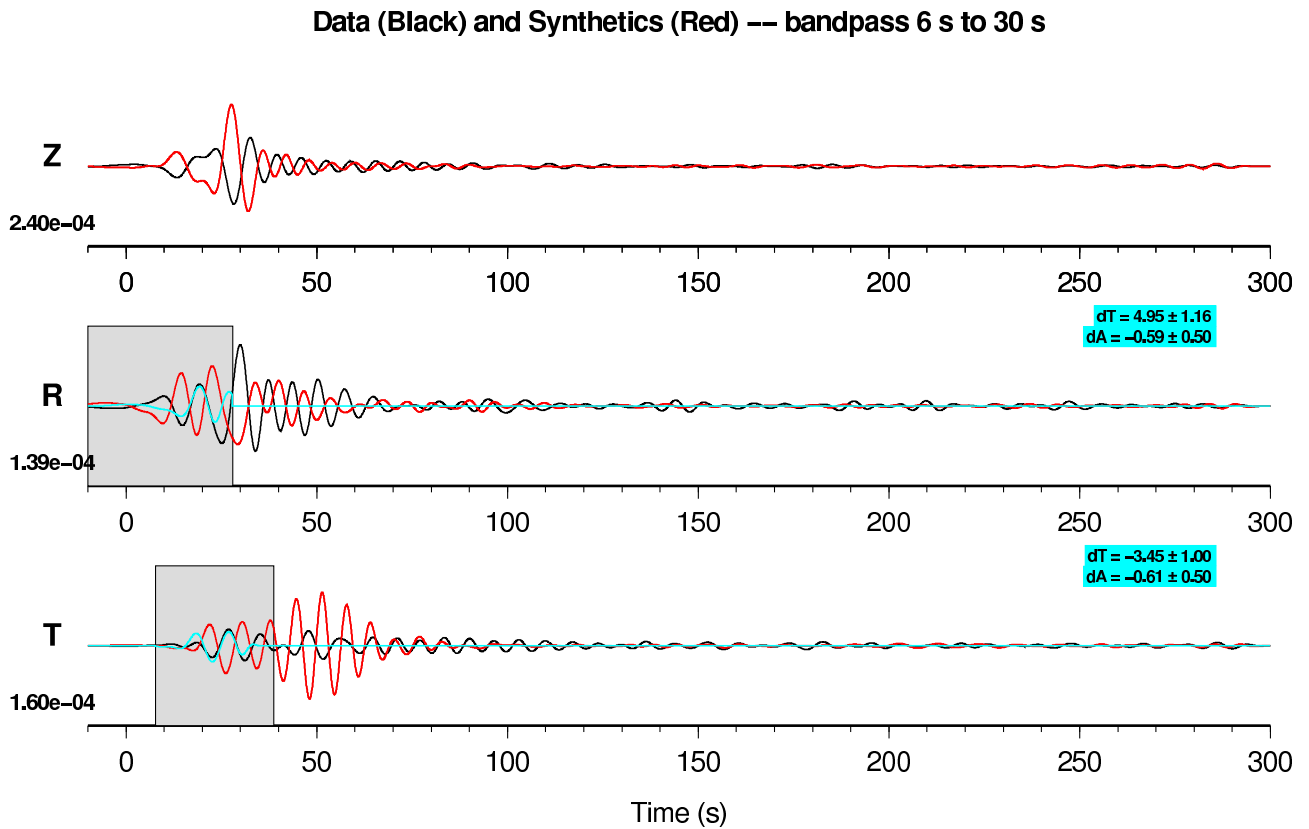
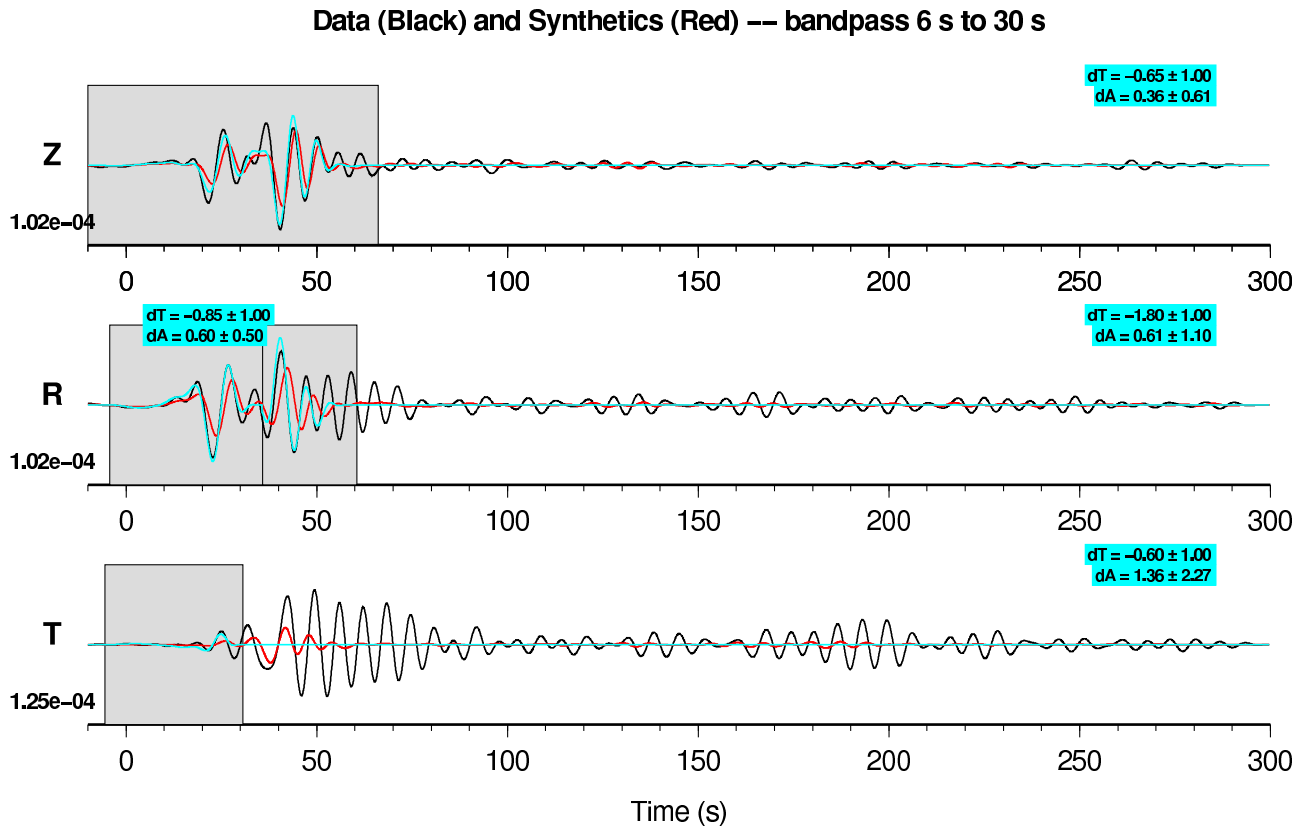


Figure E.6: Data (black) and synthetics (red), 6–30 s, from 14179736 to BVDA2.AZ. The measurement algorithm mistakenly selects the large time shifts for the Rayleigh wave, but this is due to the station error, not to the source or structure. Compare with Figure E.5.



2008 . 12 . 06
 14408052
 Mw = 4.91
 depth = 7.30 km
 MSJ . CI
 dist = 122.4 km
 az = 204.5 deg
 --
 bp [6 s, 30 s]
 model m14

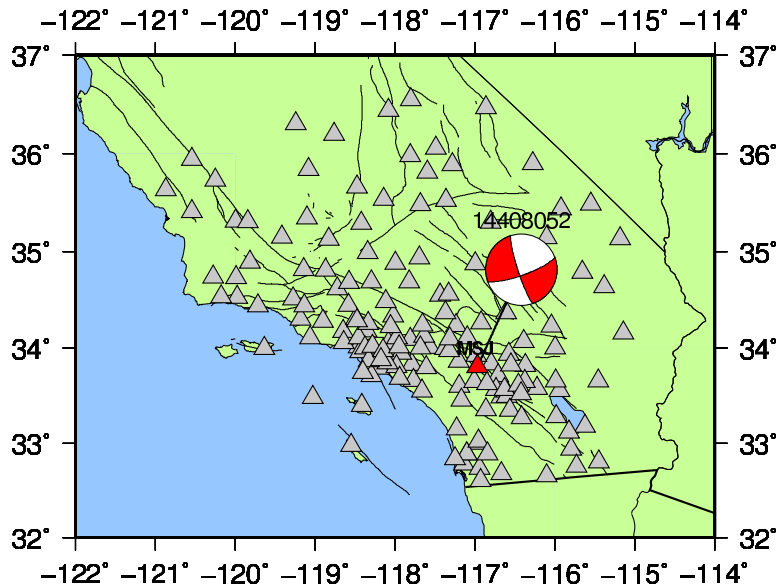
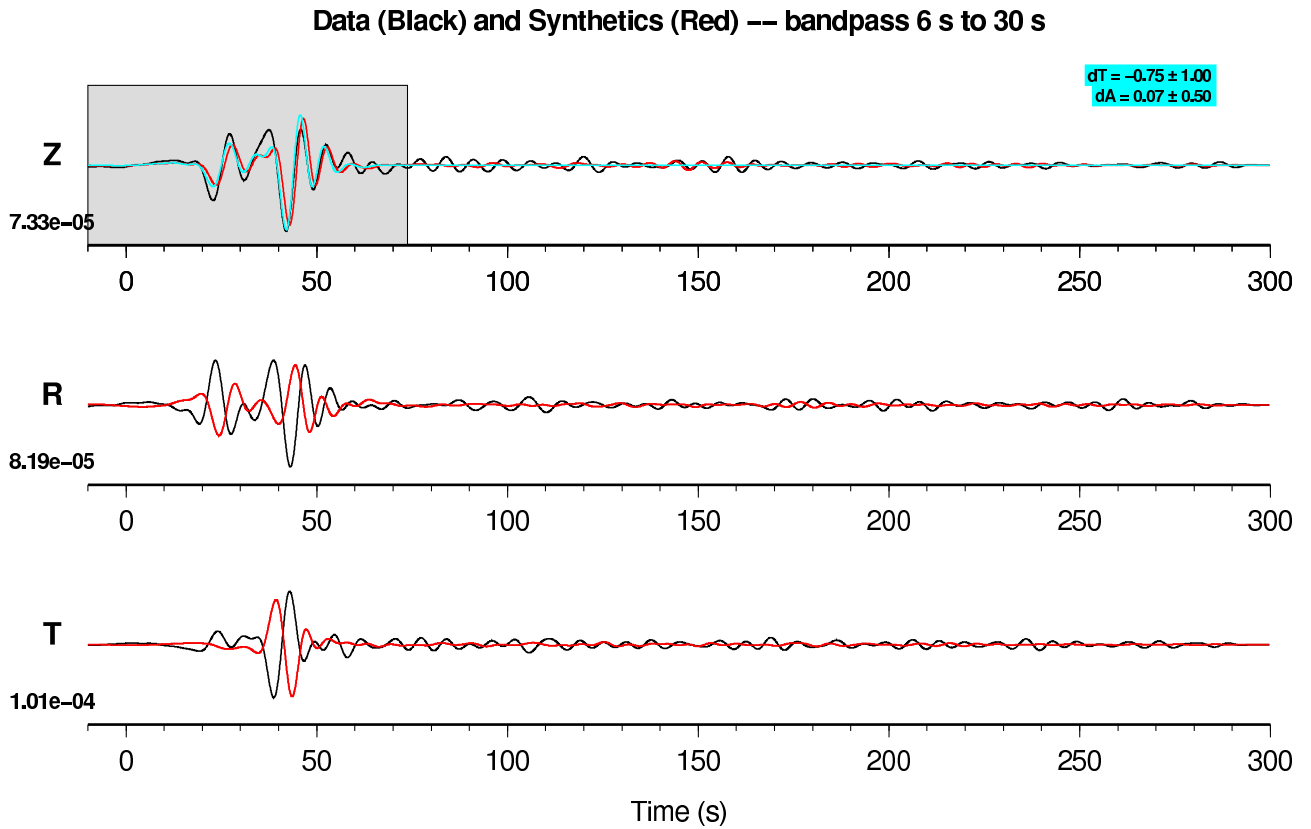


Figure E.7: Data (black) and synthetics (red), 6–30 s, from 14408052 to MSJ.CI. Compare with Figure E.8.



2008 . 12 . 06
 14408052
 Mw = 4.91
 depth = 7.30 km
 PER . CI
 dist = 128.0 km
 az = 214.7 deg
 --
 bp [6 s, 30 s]
 model m14

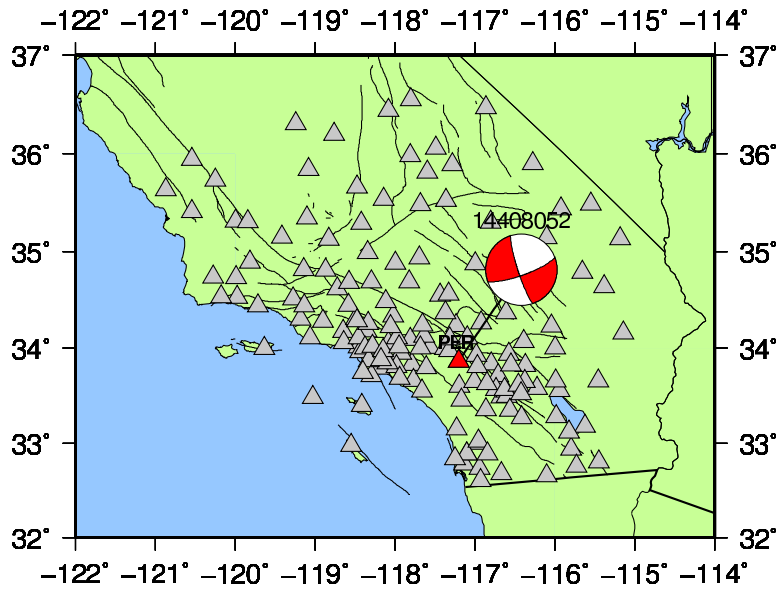
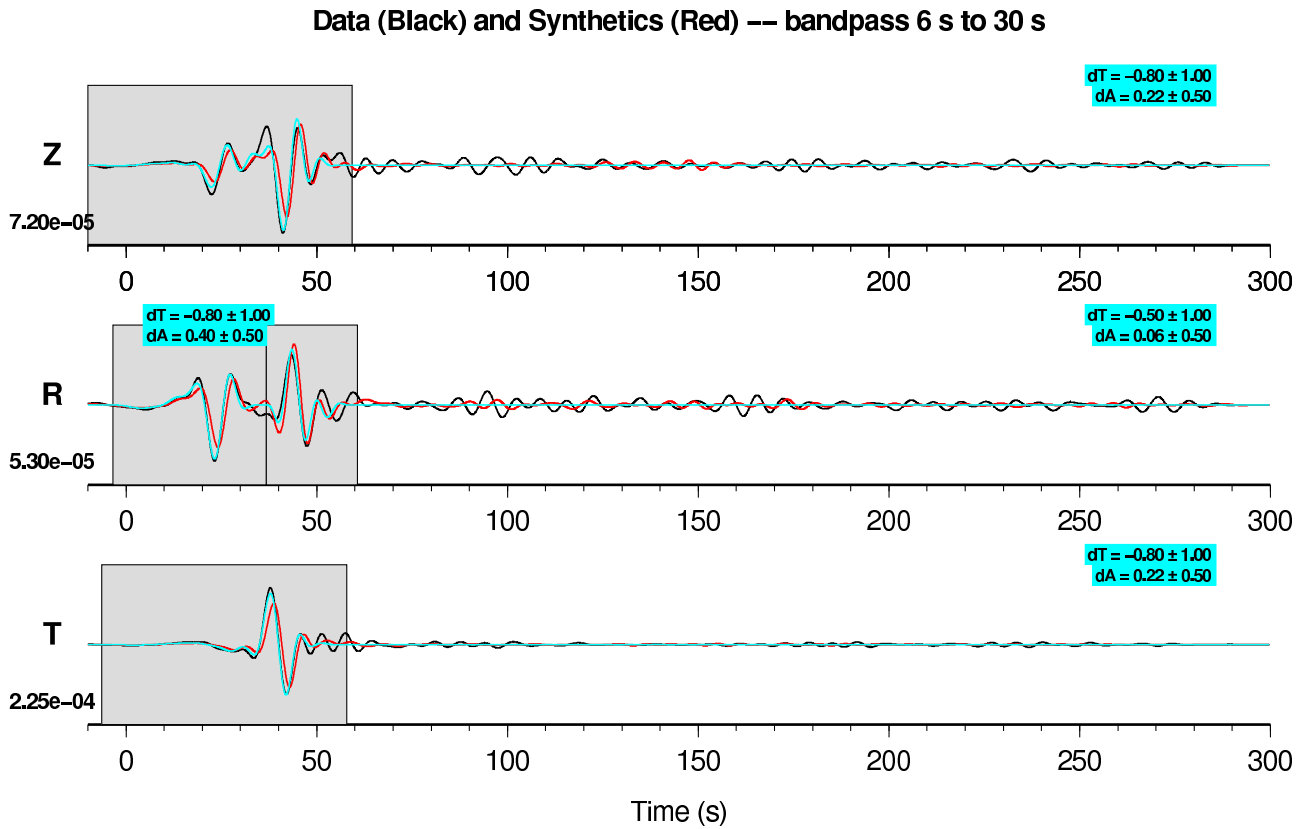


Figure E.8: Data (black) and synthetics (red), 6–30 s, from 14408052 to PER.CI. Compare with Figures E.7 and E.9.



2008 . 12 . 06
 14408052
 Mw = 4.91
 depth = 7.30 km
 RVR . CI
 dist = 126.5 km
 az = 224.3 deg
 --
 bp [6 s, 30 s]
 model m14

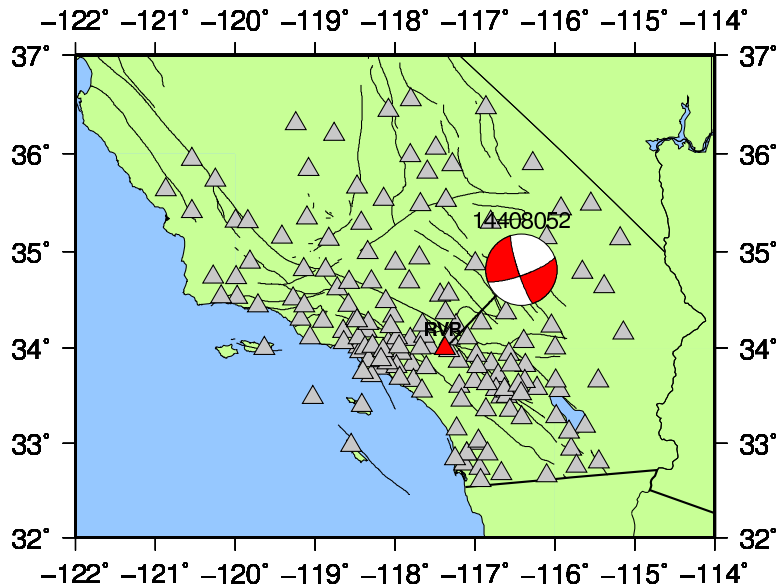
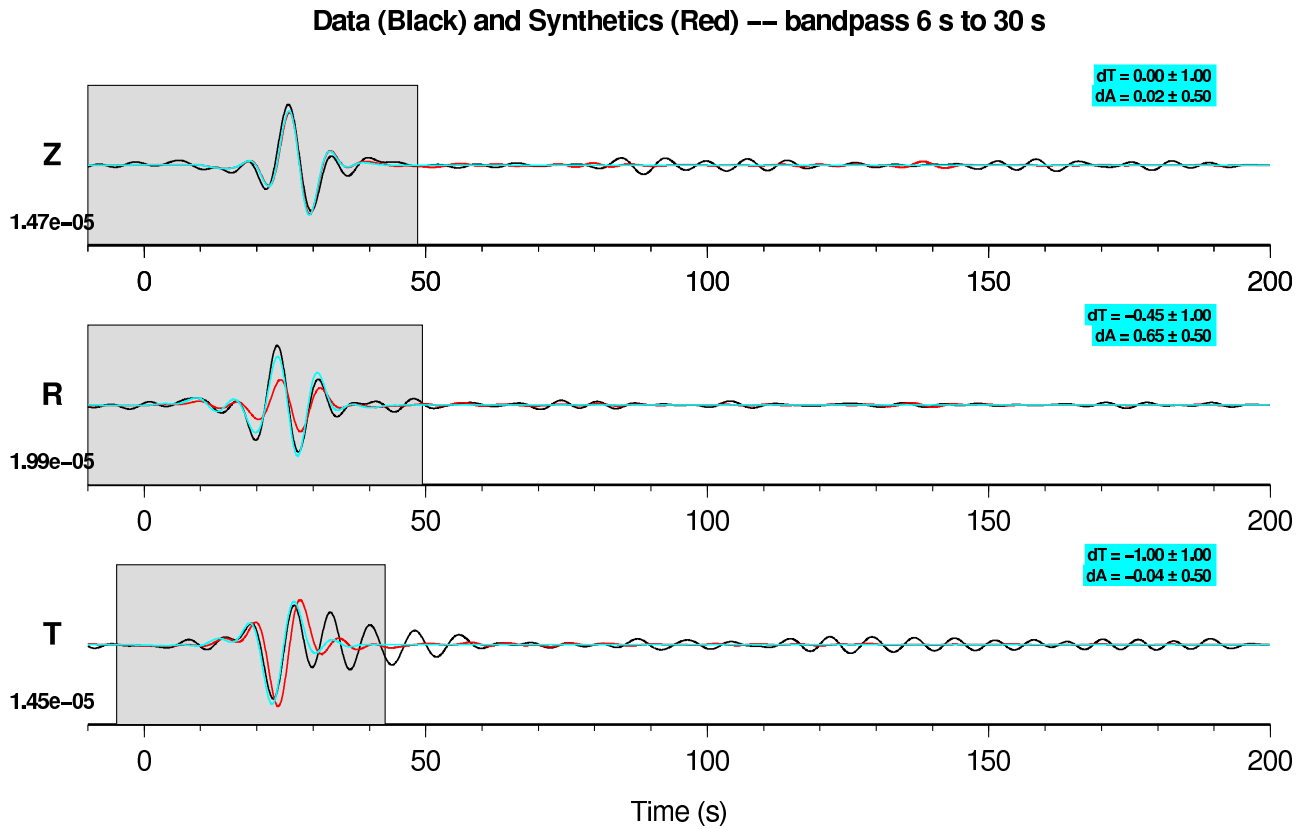


Figure E.9: Data (black) and synthetics (red), 6–30 s, from 14408052 to RVR.CI. Compare with Figure E.8.



2003 . 01 . 25
 9882329
 Mw = 4.20
 depth = 4.12 km
 ALP . CI
 dist = 76.8 km
 az = 154.6 deg
 --
 bp [6 s, 30 s]
 model m15

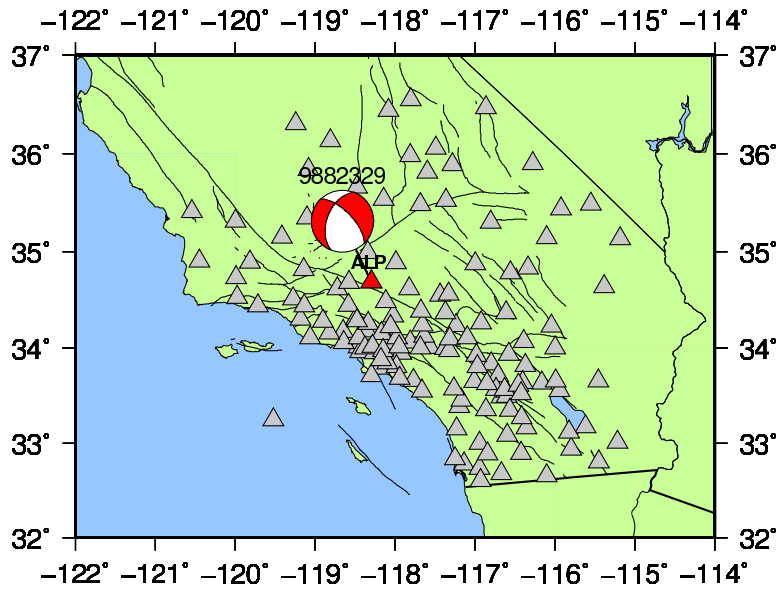


Figure E.10: Data (black) and synthetics (red), 6–30 s, from 14138080 to ALP.CI. Compare with Figure E.11.

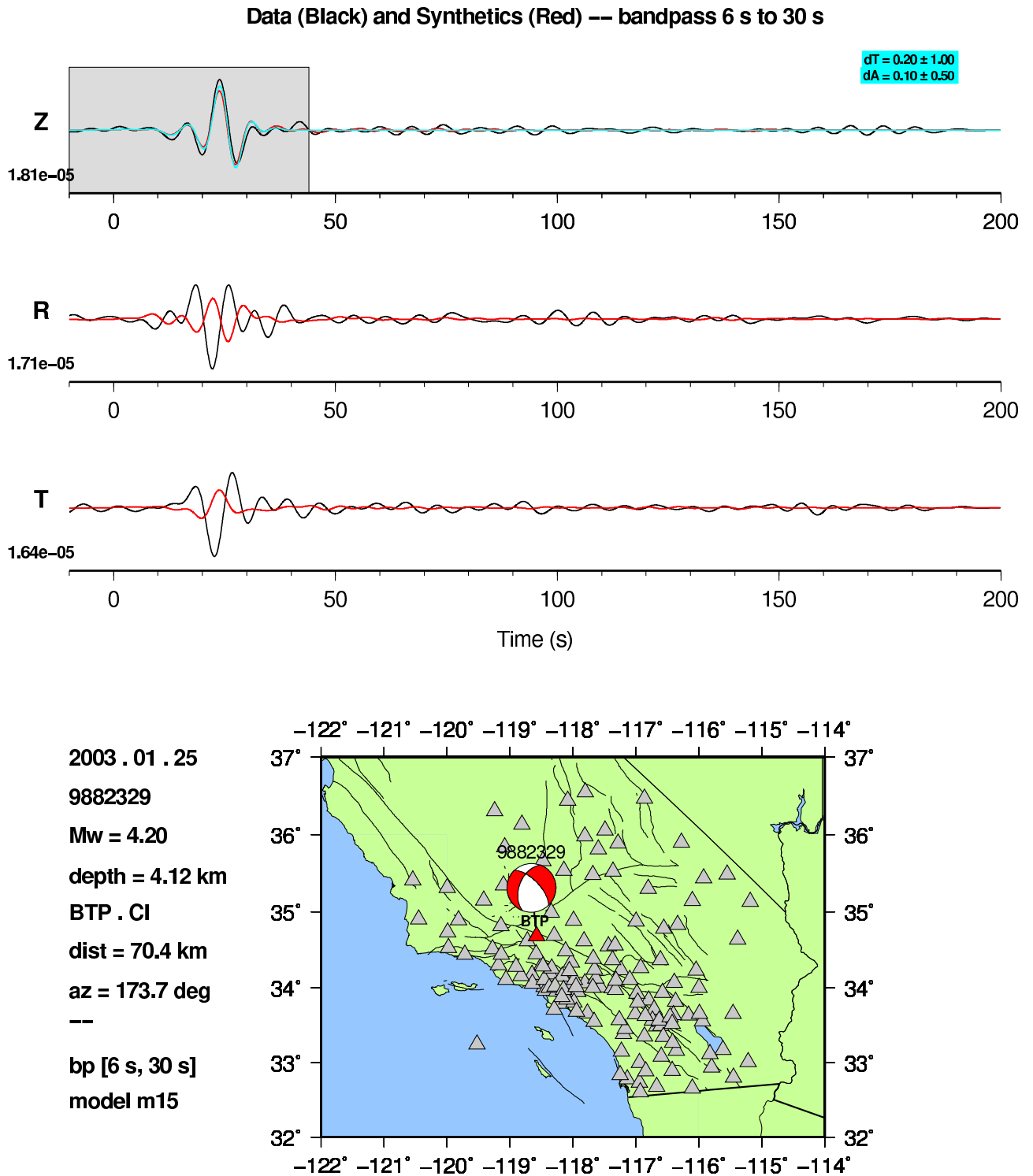
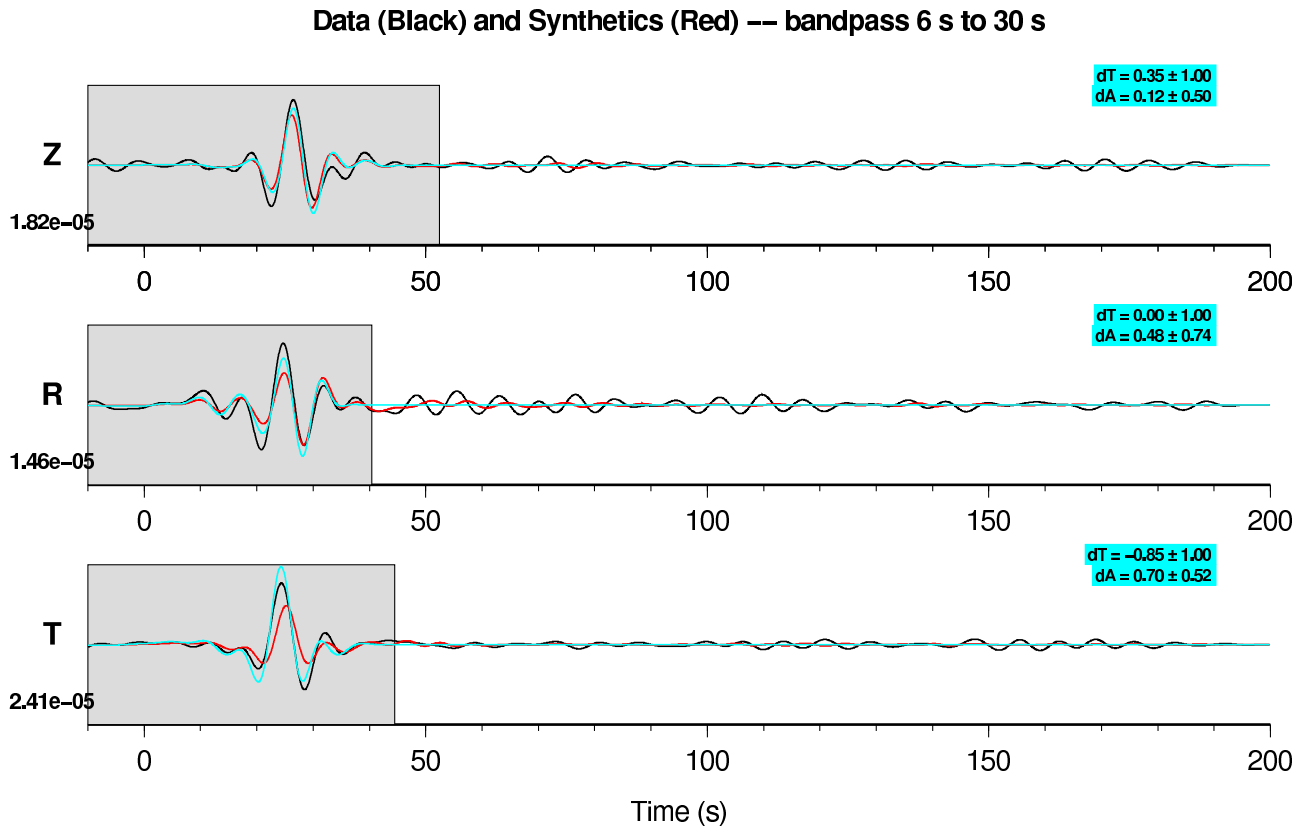


Figure E.11: Data (black) and synthetics (red), 6–30 s, from 14138080 to BTP.CI. Compare with Figures E.10 and E.12.



2003 . 01 . 25
 9882329
 Mw = 4.20
 depth = 4.12 km
 OSI . CI
 dist = 77.7 km
 az = 184.4 deg
 --
 bp [6 s, 30 s]
 model m15

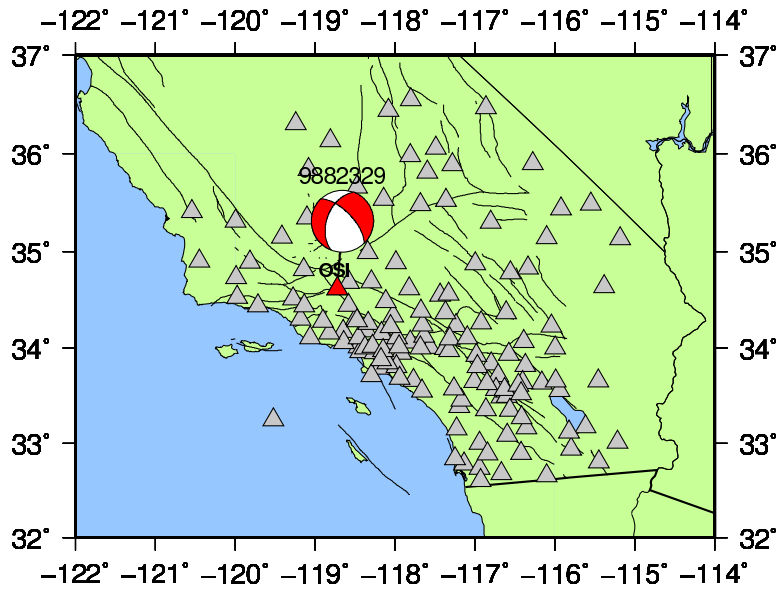
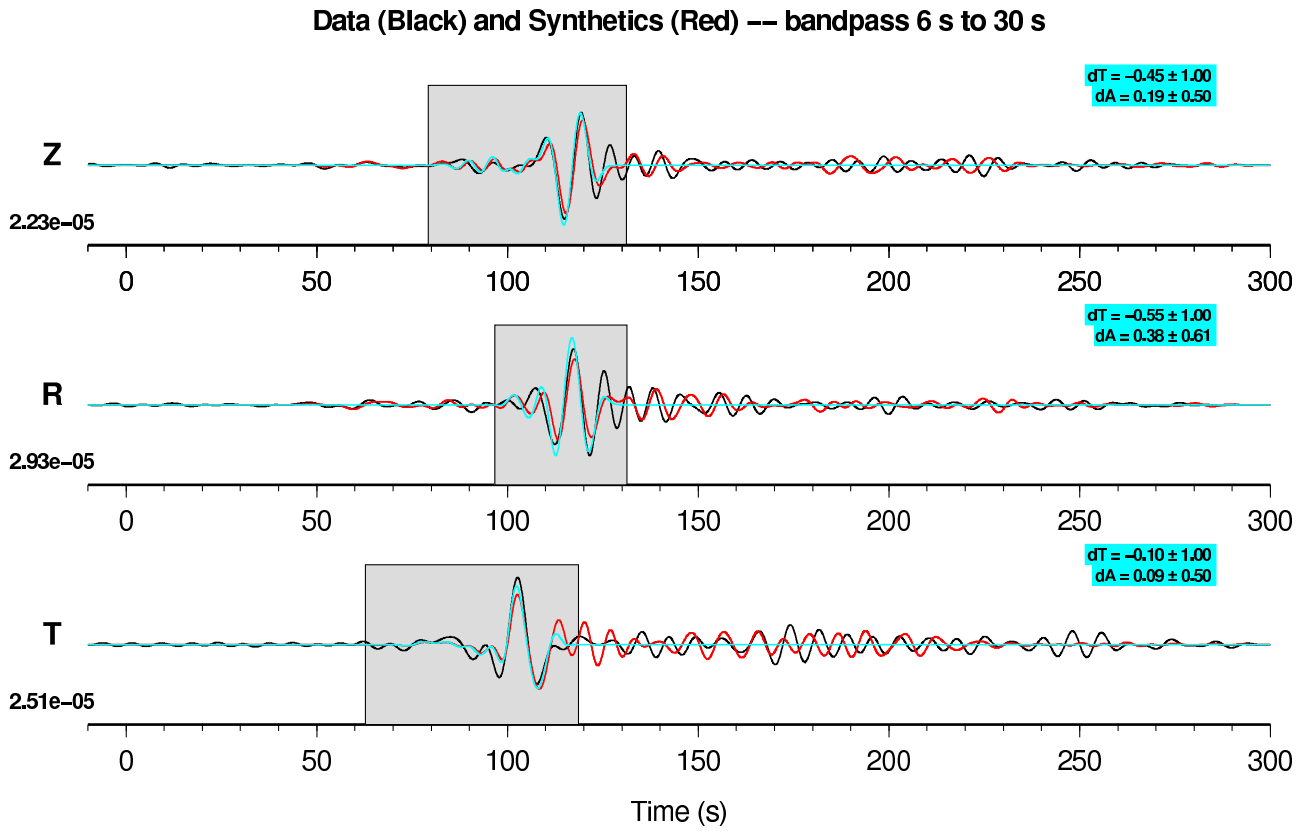


Figure E.12: Data (black) and synthetics (red), 6–30 s, from 14138080 to OSI.CI. Compare with Figure E.11.



2005 . 04 . 16
 14138080
 Mw = 4.56
 depth = 10.16 km
 CTC . CI
 dist = 330.4 km
 az = 115.9 deg
 --
 bp [6 s, 30 s]
 model m16

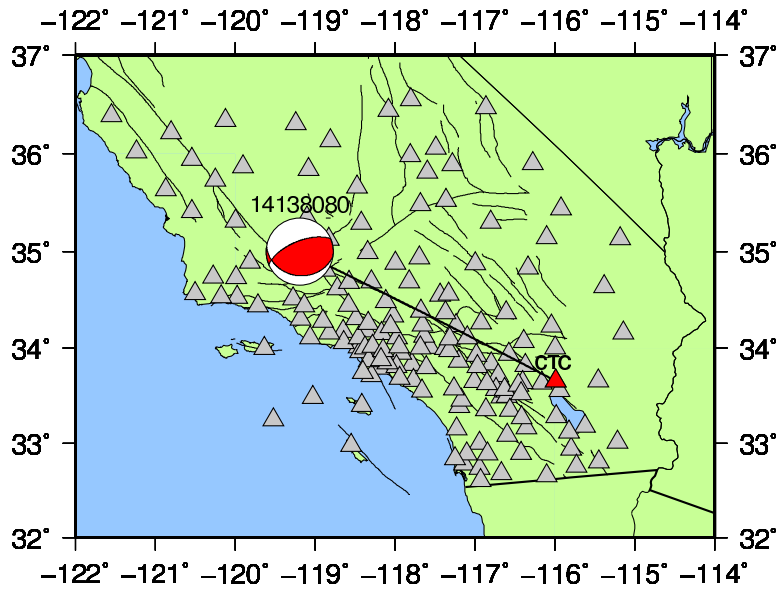


Figure E.13: Data (black) and synthetics (red), 6–30 s, from 14138080 to CTC.CI. Compare with Figure E.14.

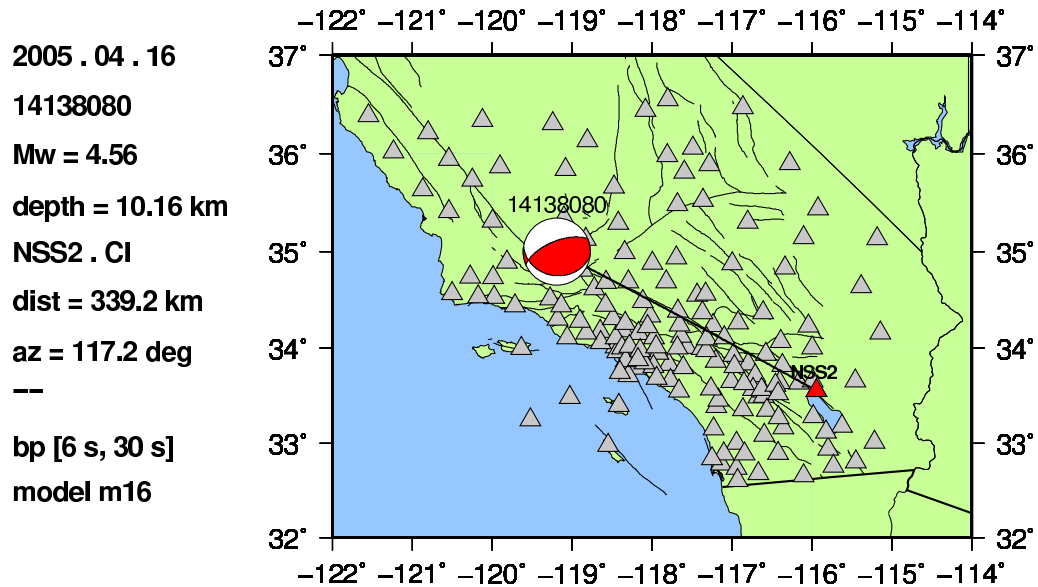
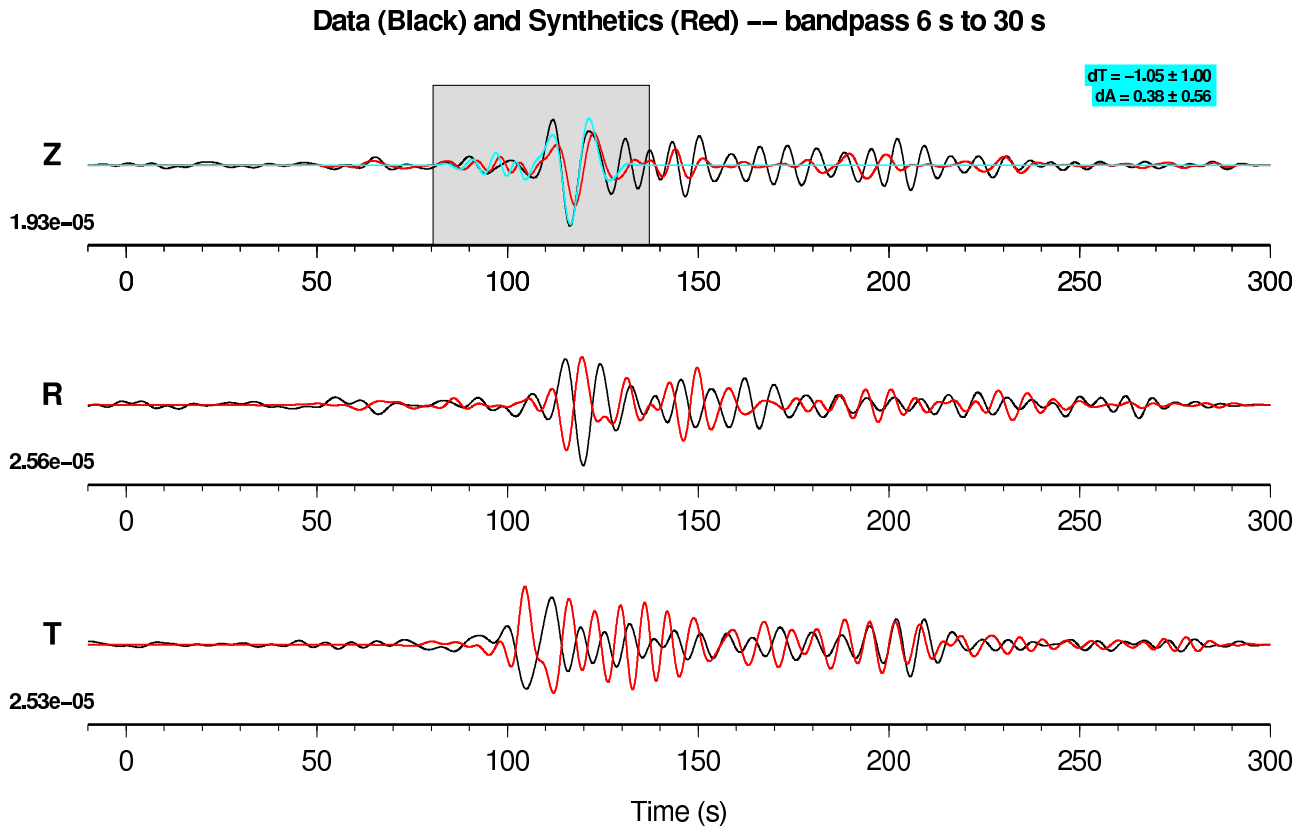
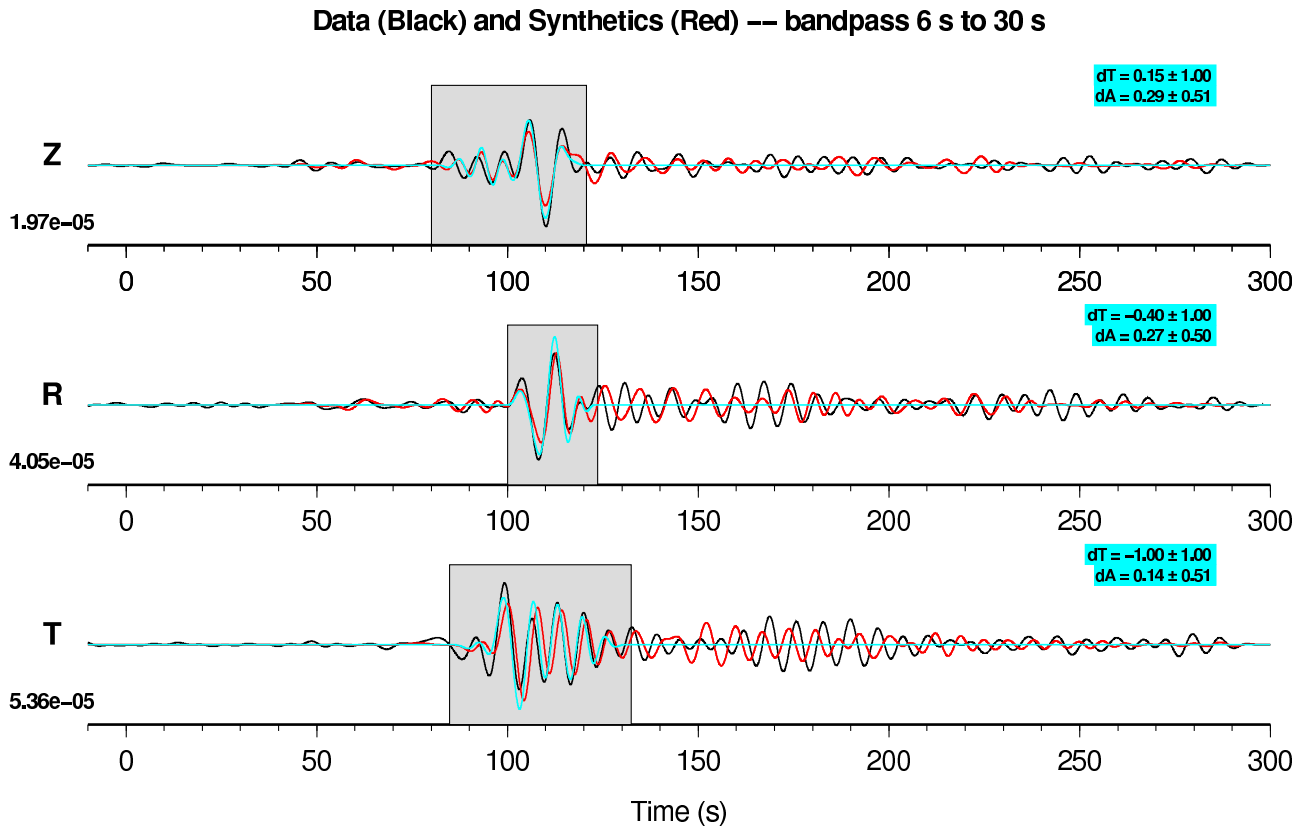


Figure E.14: Data (black) and synthetics (red), 6–30 s, from 14138080 to NSS2.CI. Compare with Figures E.13 and E.15.



2005 . 04 . 16
 14138080
 Mw = 4.56
 depth = 10.16 km
 THX . CI
 dist = 317.2 km
 az = 117.6 deg
 --
 bp [6 s, 30 s]
 model m16

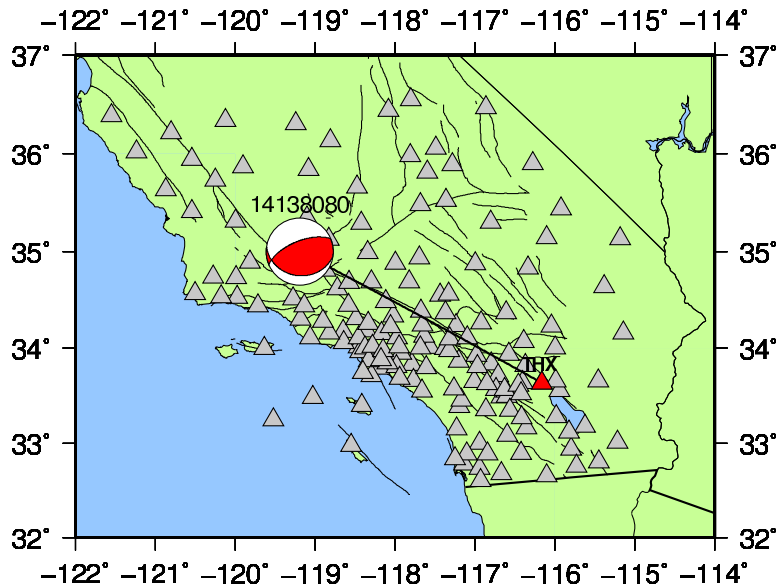
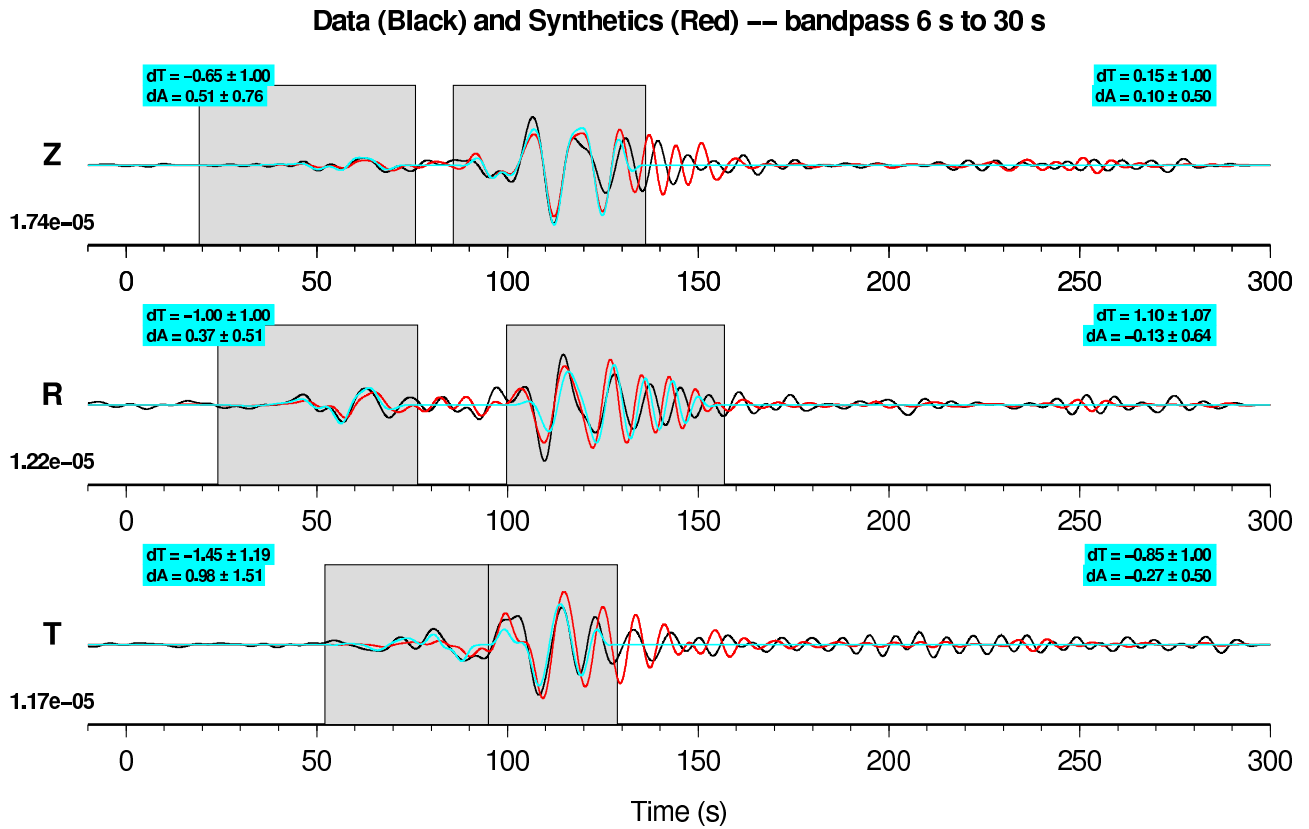


Figure E.15: Data (black) and synthetics (red), 6–30 s, from 14138080 to THX.CI. Compare with Figure E.14.



2005 . 04 . 16
 14138080
 Mw = 4.56
 depth = 10.54 km
 SDR . CI
 dist = 326.2 km
 az = 139.7 deg
 --
 bp [6 s, 30 s]
 model m16

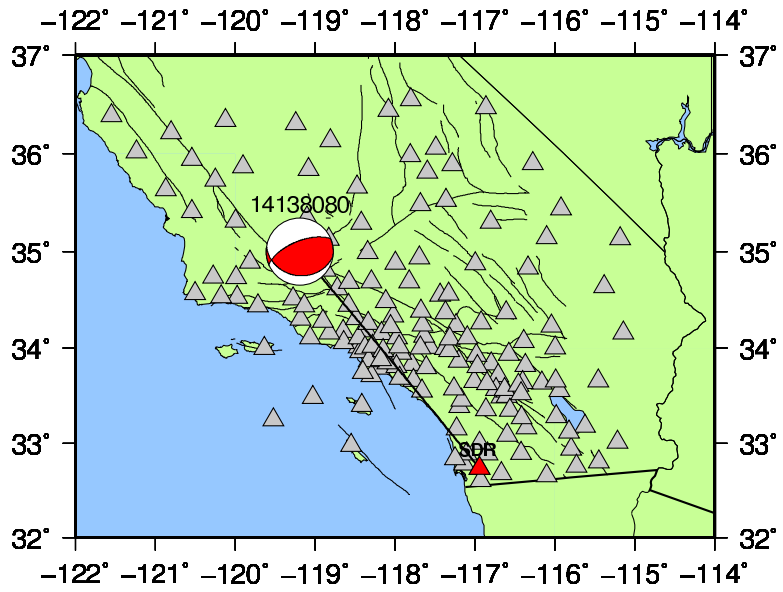
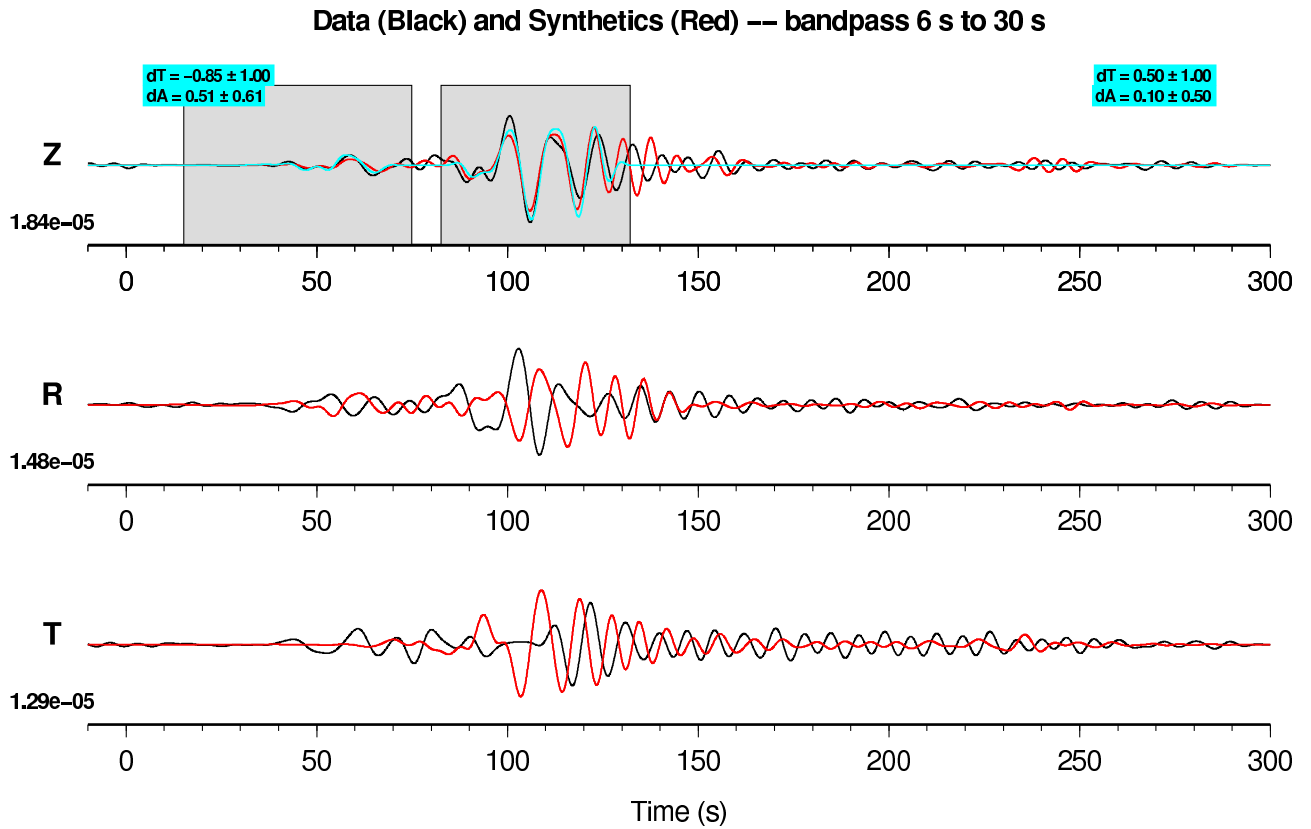


Figure E.16: Data (black) and synthetics (red), 6–30 s, from 14138080 to SDR.CI. Compare with Figure E.17.



2005 . 04 . 16
 14138080
 Mw = 4.56
 depth = 10.54 km
 109C . TA
 dist = 303.4 km
 az = 139.9 deg
 --
 bp [6 s, 30 s]
 model m16

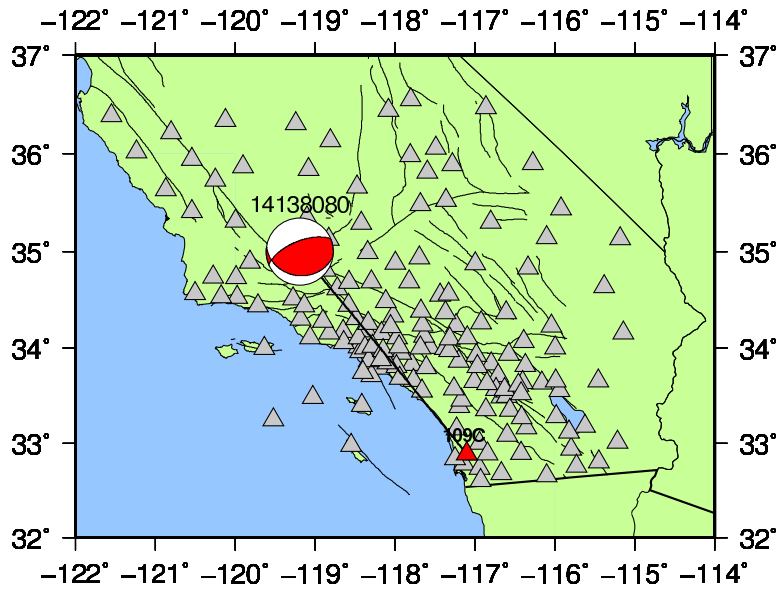
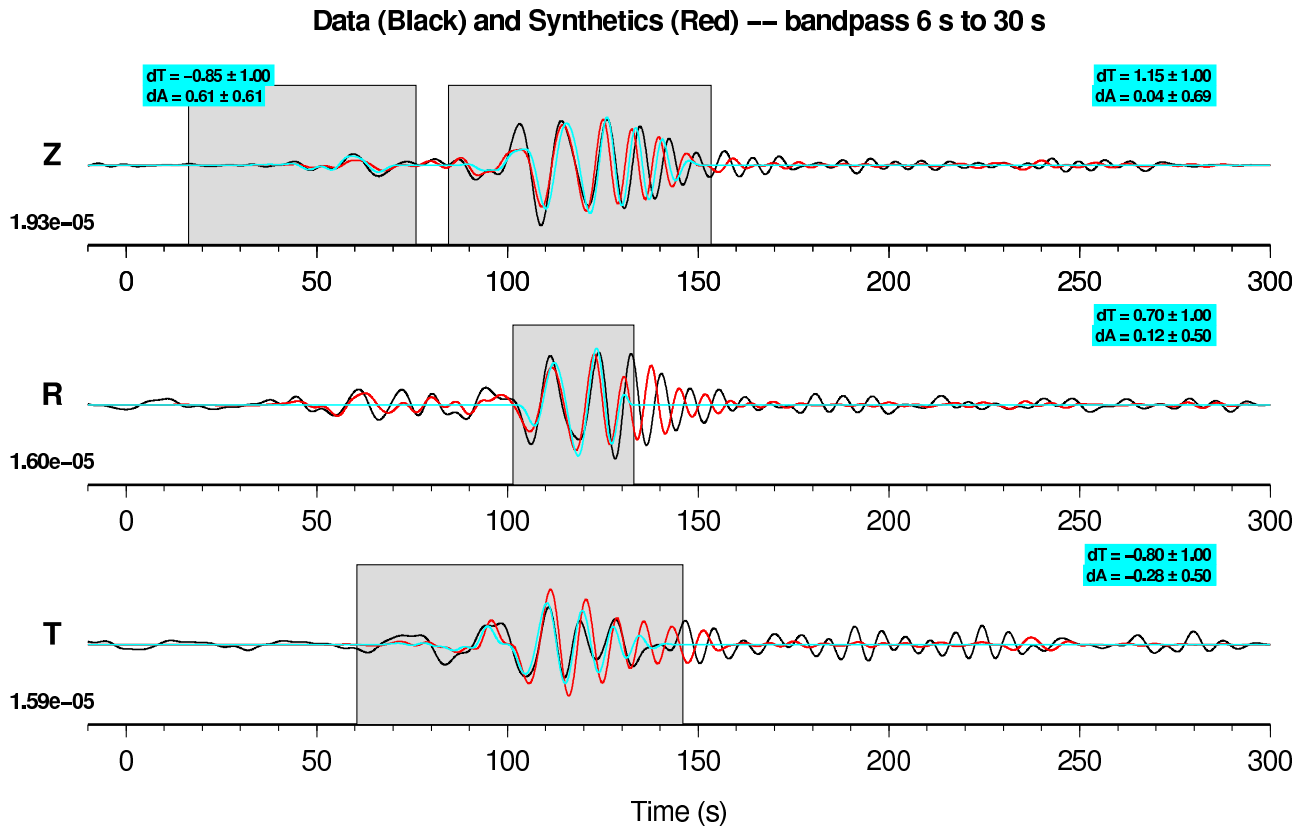


Figure E.17: Data (black) and synthetics (red), 6–30 s, from 14138080 to 109C.TA. Compare with Figures E.16 and E.18.



2005 . 04 . 16
 14138080
 Mw = 4.56
 depth = 10.54 km
 SDG . CI
 dist = 310.7 km
 az = 141.7 deg
 --
 bp [6 s, 30 s]
 model m16

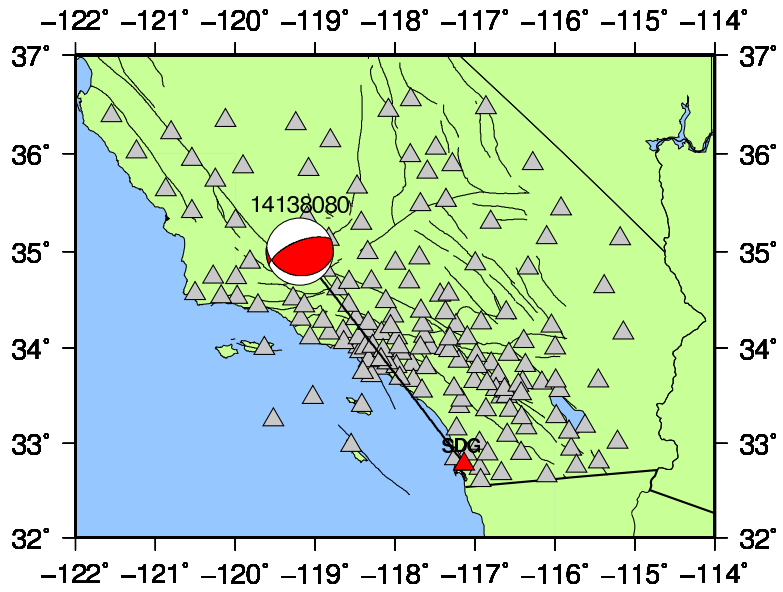


Figure E.18: Data (black) and synthetics (red), 6–30 s, from 14138080 to SDG.CI. Compare with Figure E.17.

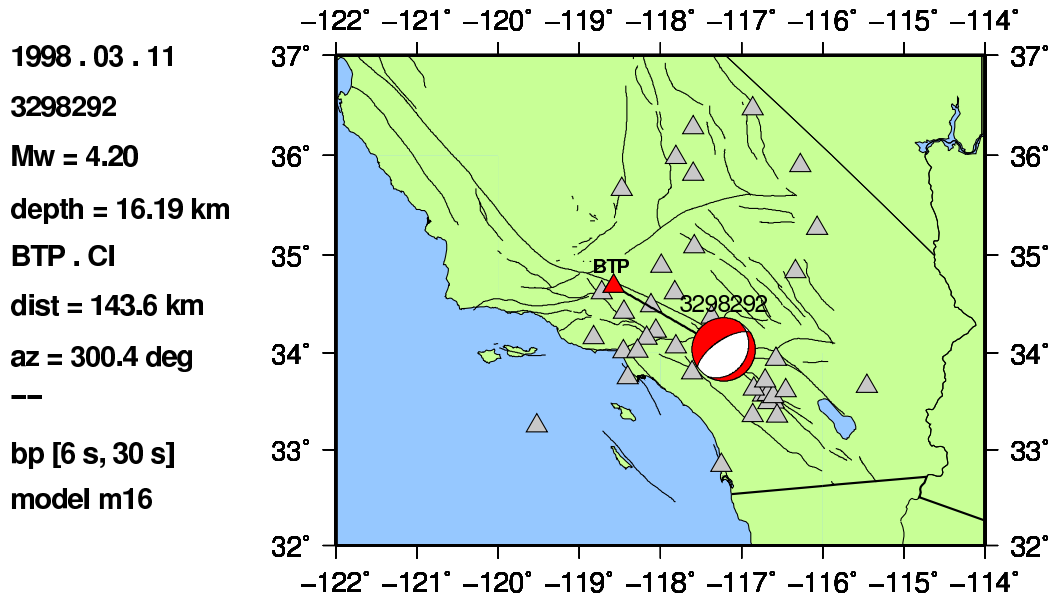
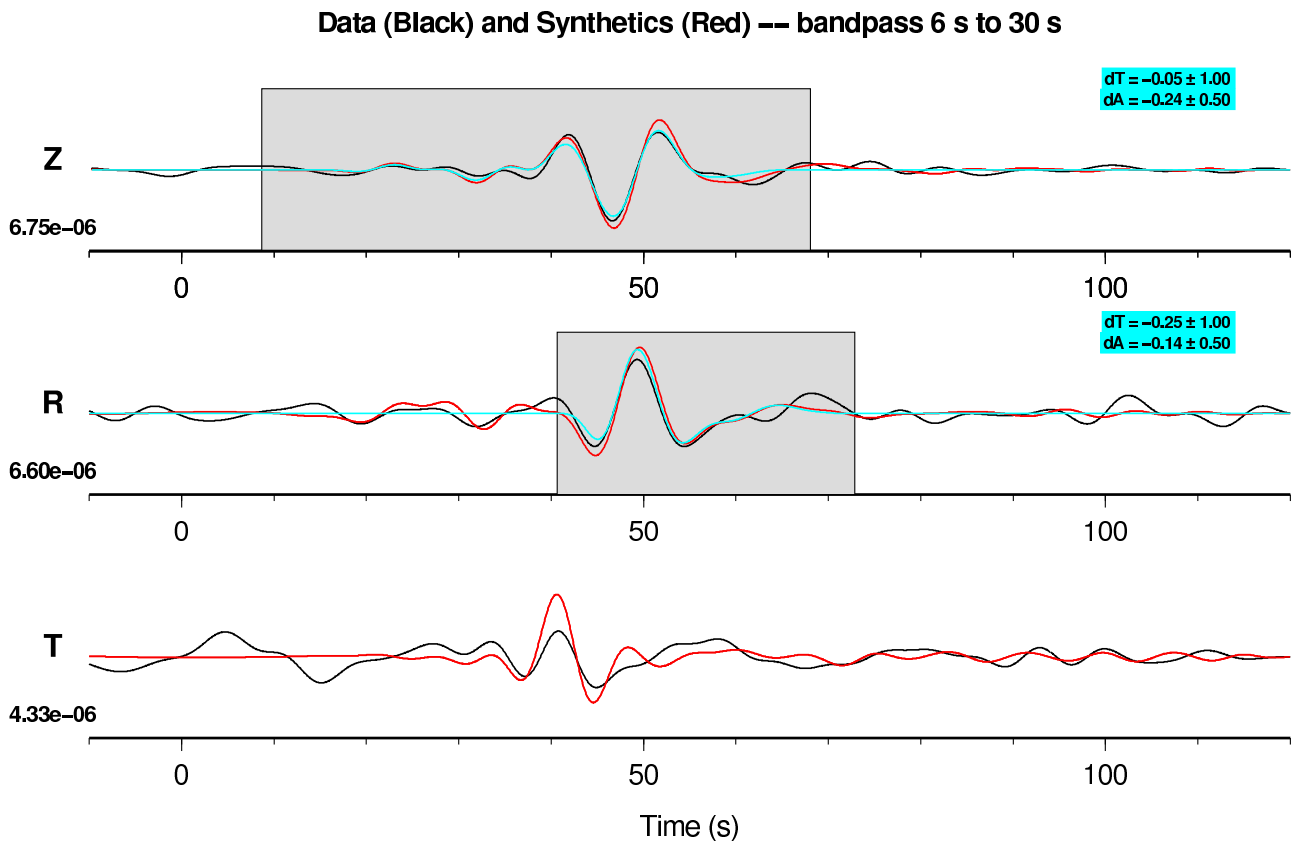


Figure E.19: Data (black) and synthetics (red), 6–30 s, from 3298292 to BTP.CI. Note that the polarity problem on this east-west-oriented path is most apparent on the radial component. Compare with Figure E.20.

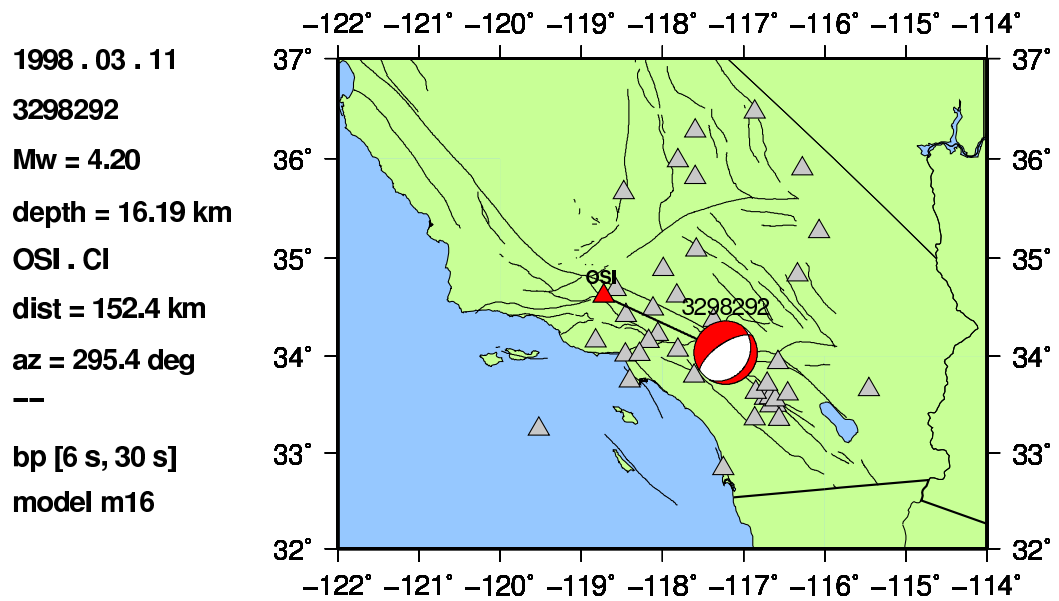
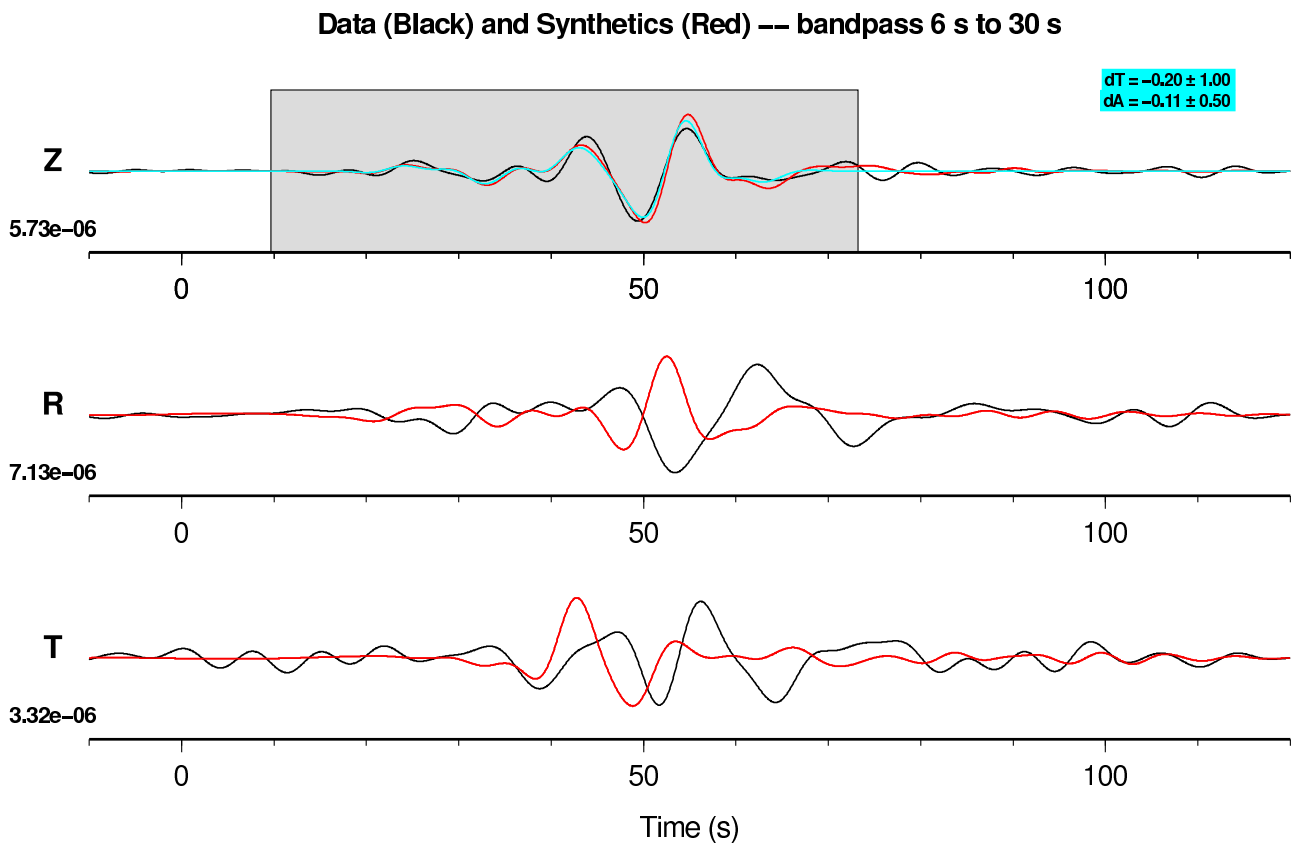


Figure E.20: Data (black) and synthetics (red), 6–30 s, from 3298292 to OSI.CI. Compare with Figure E.12.

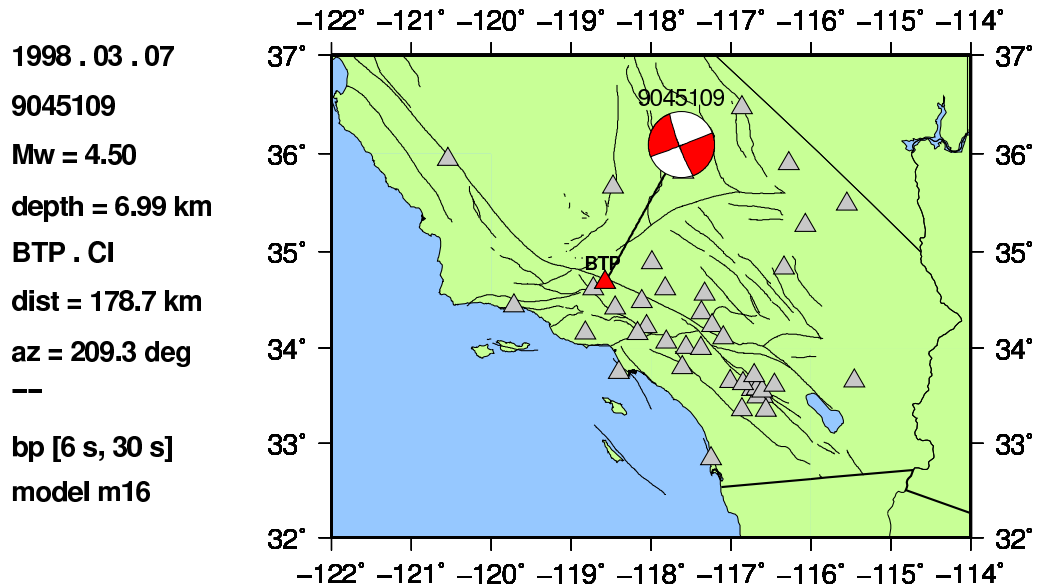
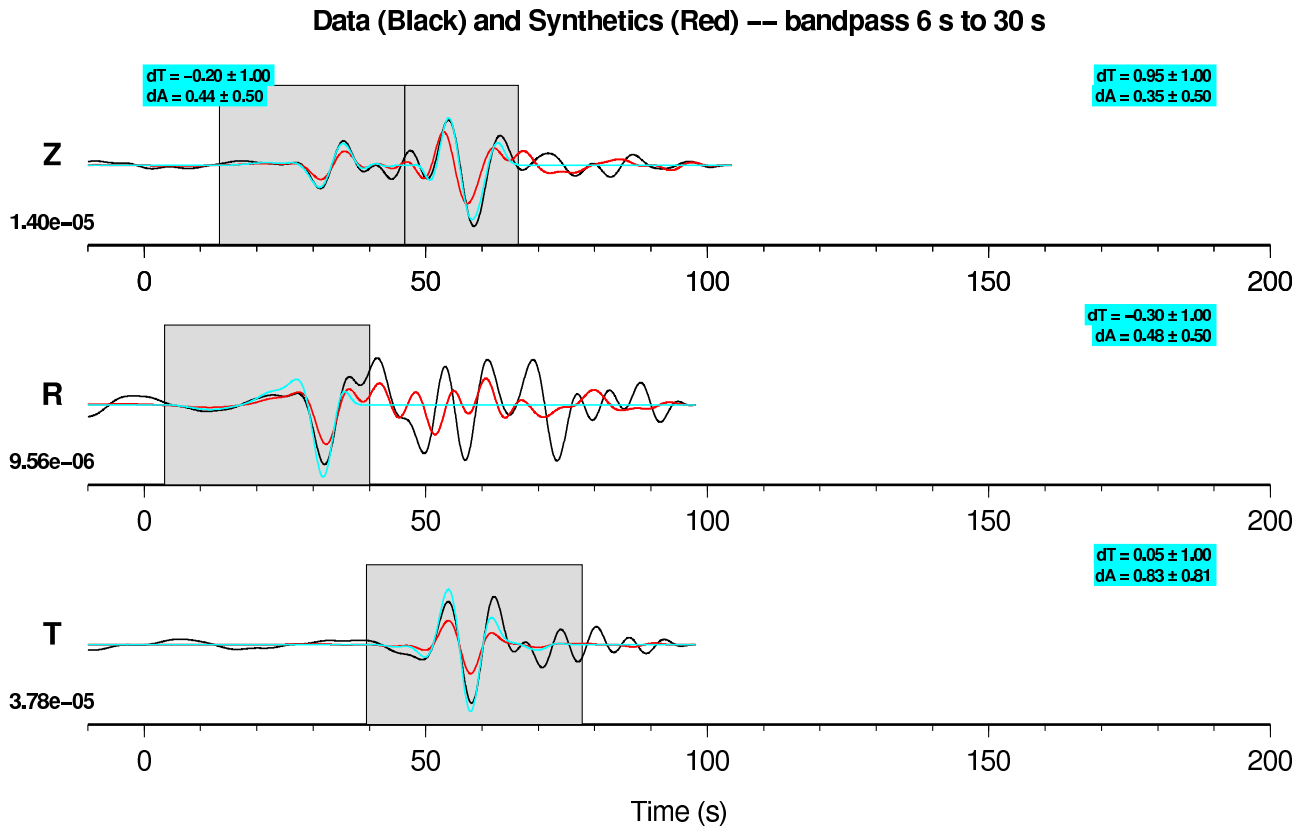


Figure E.21: Data (black) and synthetics (red), 6–30 s, from 9045109 to BTP.CI. Compare with Figure E.22.

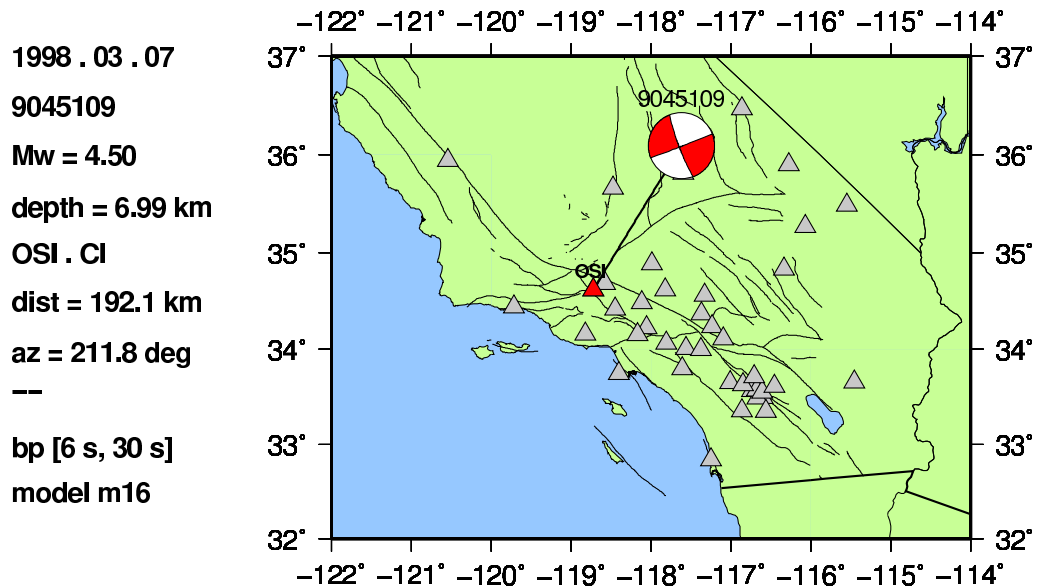
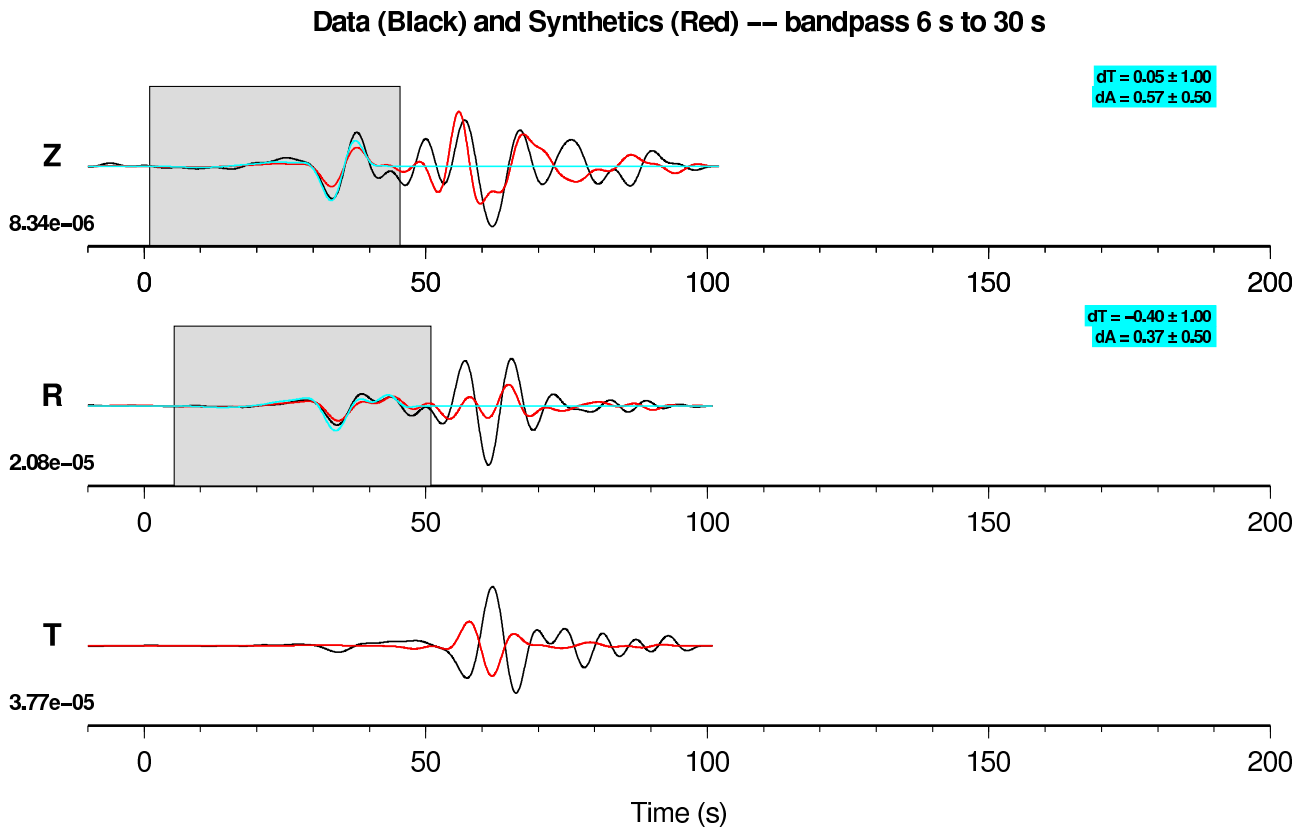
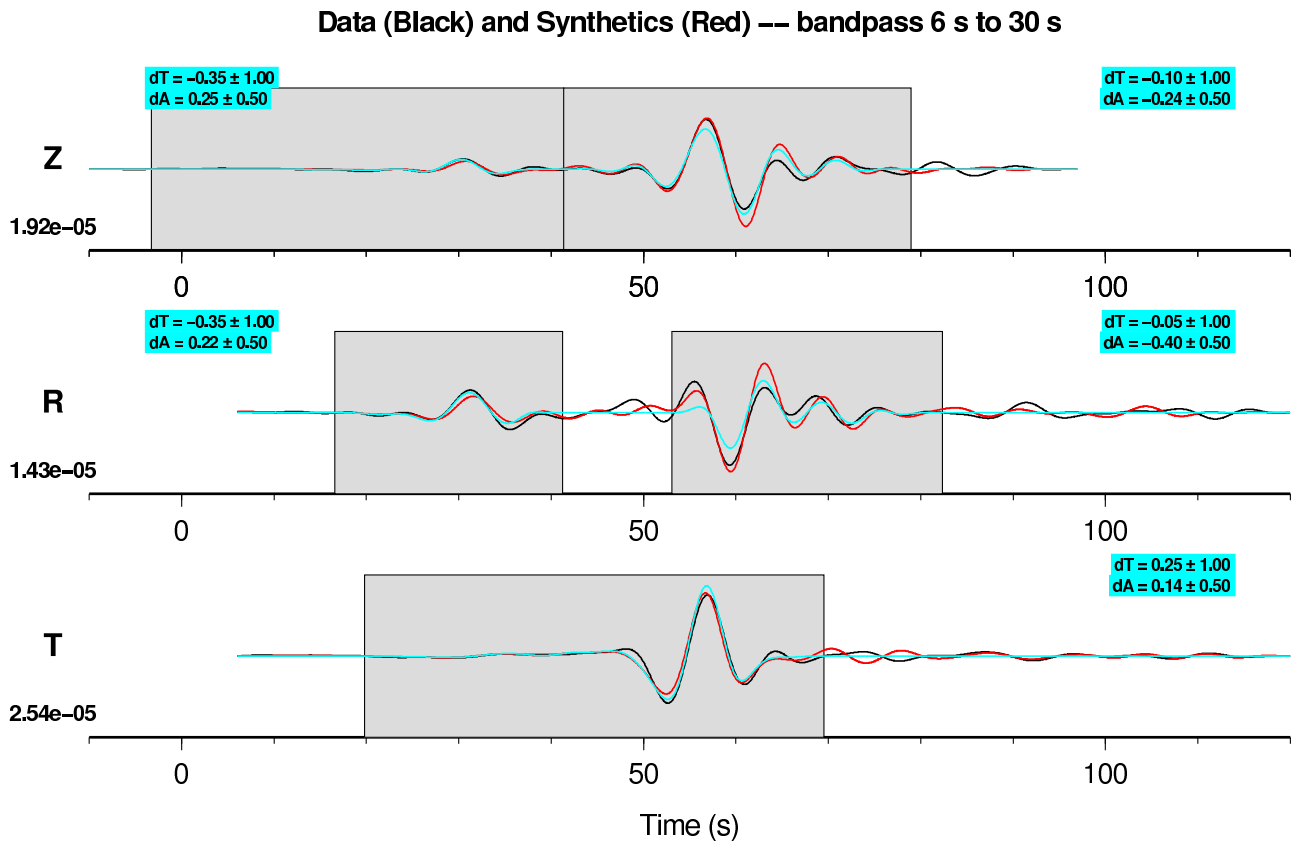


Figure E.22: Data (black) and synthetics (red), 6–30 s, from 9045109 to OSI.CI. Note that the polarity problem on this north-south-oriented path is most apparent on the transverse component. Compare with Figure E.21.



1998 . 08 . 16
 9064093
 Mw = 4.40
 depth = 5.98 km
 OSI . CI
 dist = 174.3 km
 az = 288.7 deg
 --
 bp [6 s, 30 s]
 model m16

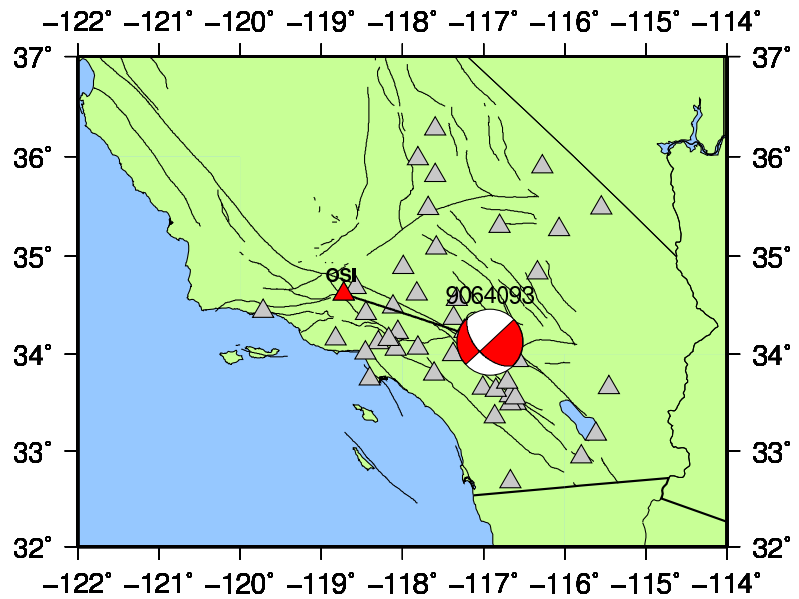
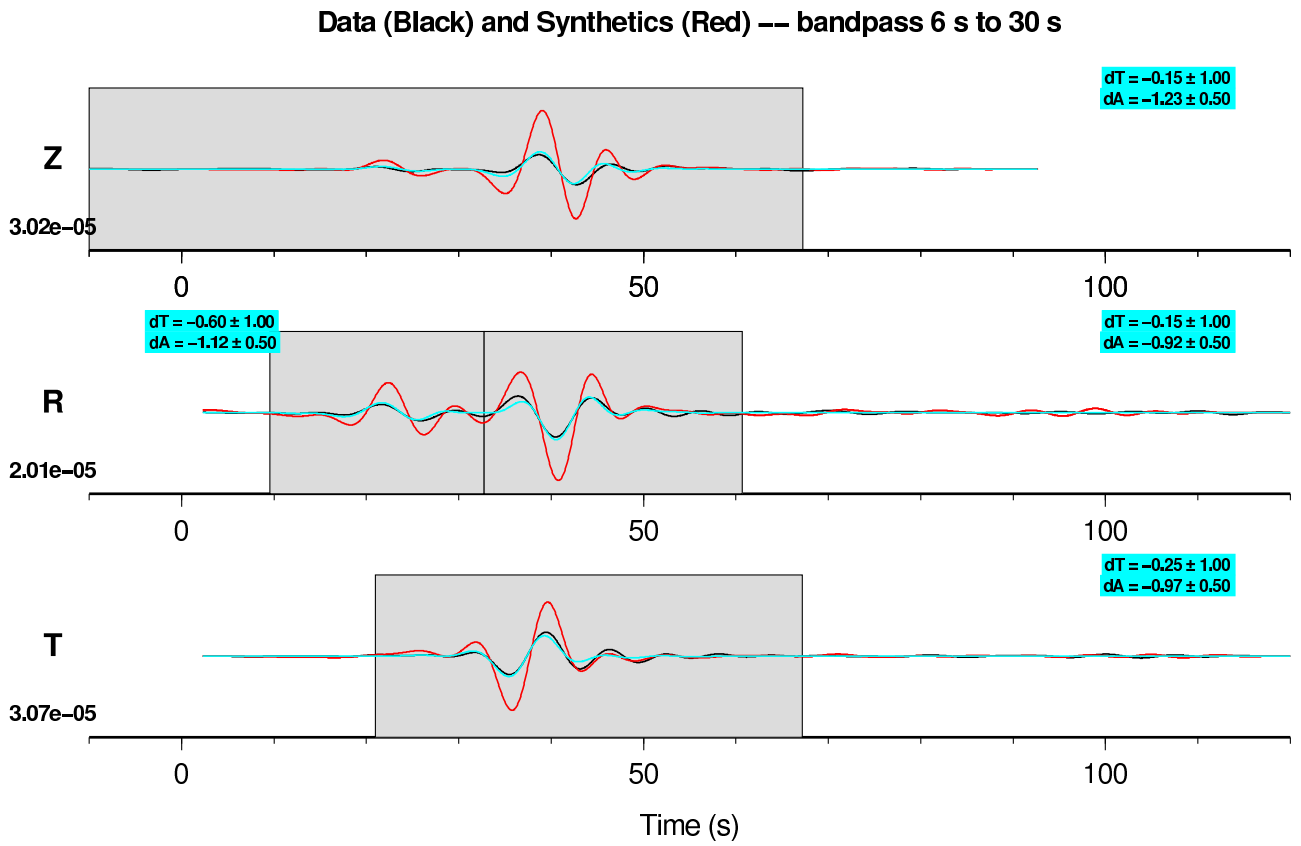


Figure E.23: Data (black) and synthetics (red), 6–30 s, from 9064093 to OSI.CI. Compare with Figure E.24.



1998 . 08 . 16
 9064093
 Mw = 4.40
 depth = 5.98 km
 VCS . CI
 dist = 117.0 km
 az = 290.2 deg
 --
 bp [6 s, 30 s]
 model m16

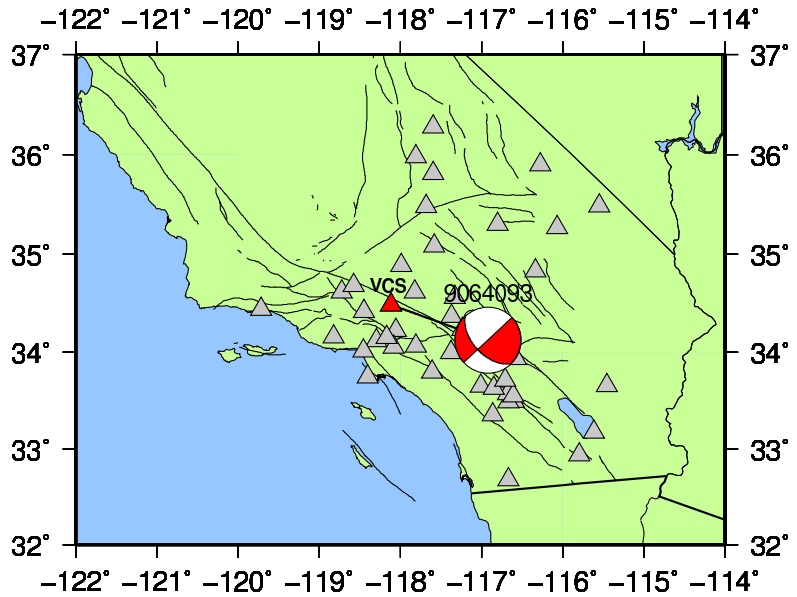


Figure E.24: Data (black) and synthetics (red), 6–30 s, from 9064093 to VCS.CI. The amplification problem is on all three components. Compare with Figures E.25 and E.23.

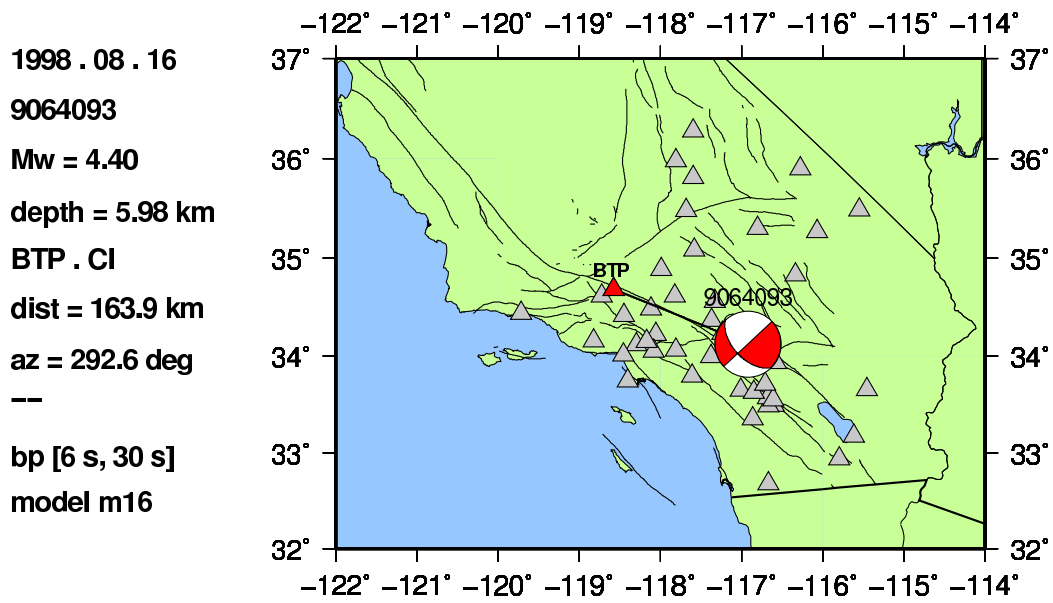
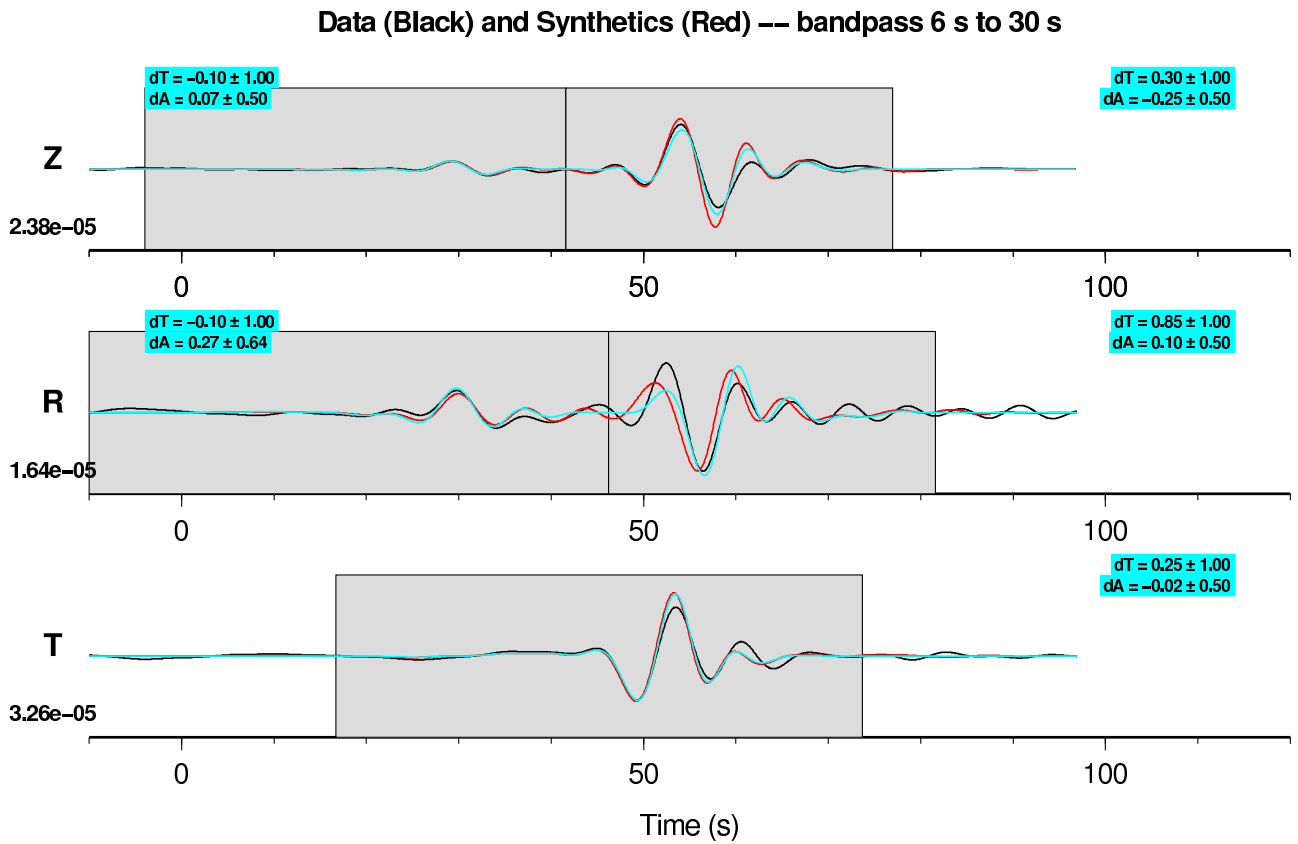
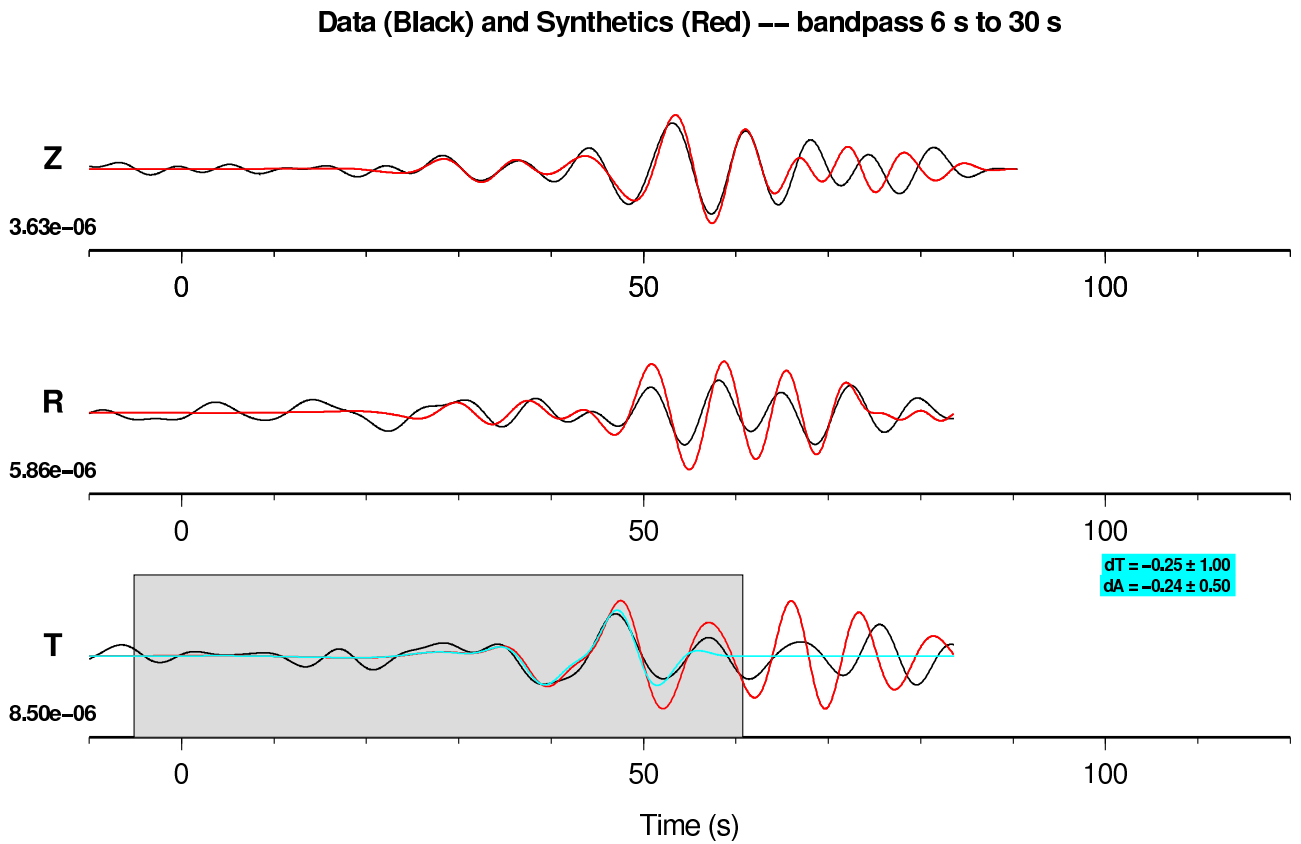


Figure E.25: Data (black) and synthetics (red), 6–30 s, from 9064093 to BTP.CI. Compare with Figure E.24.



1999 . 05 . 14
 9086693
 Mw = 3.90
 depth = 3.98 km
 SWS . CI
 dist = 132.5 km
 az = 156.4 deg
 --
 bp [6 s, 30 s]
 model m16

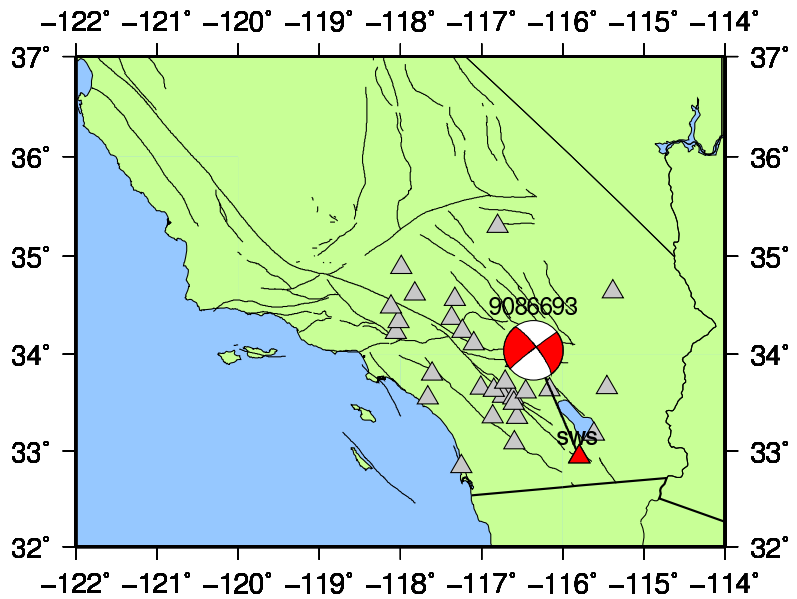
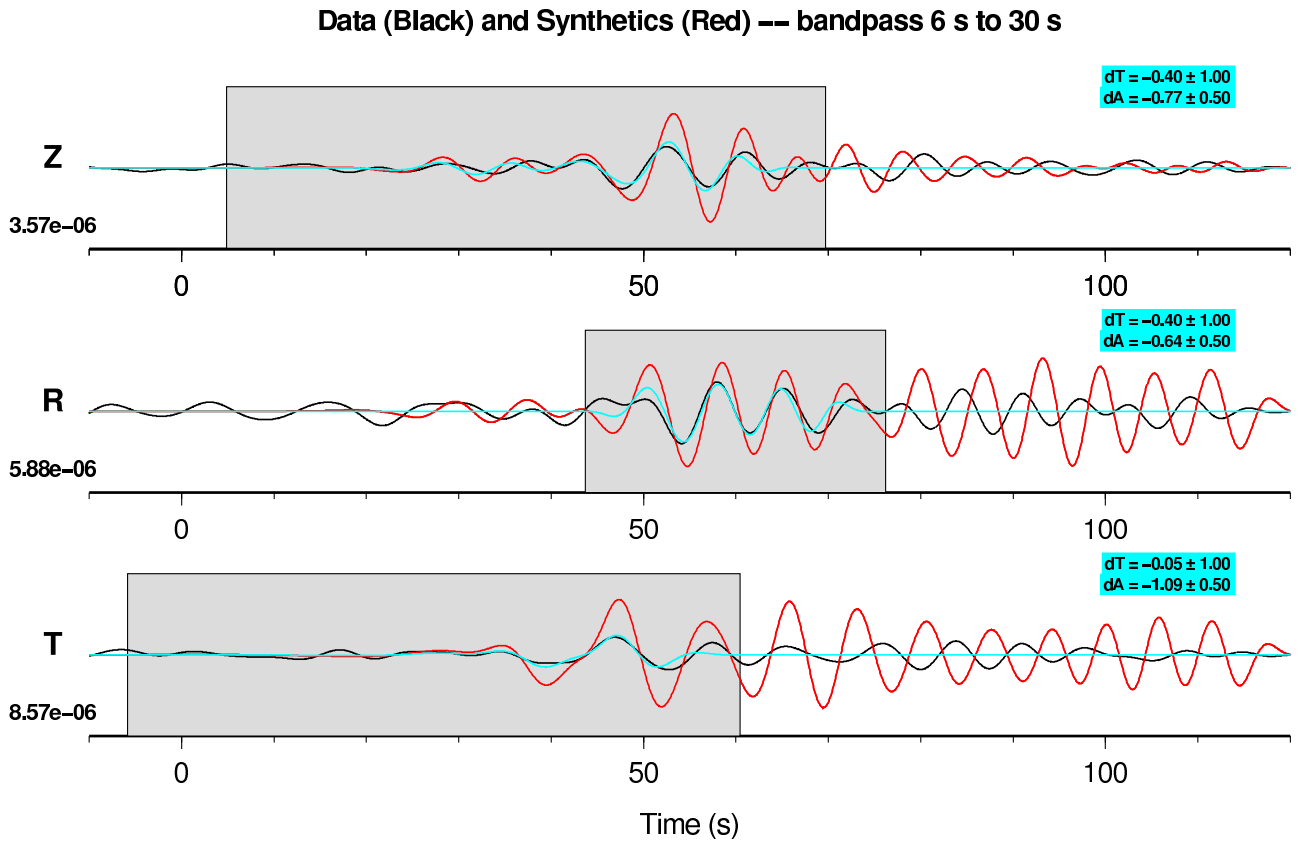


Figure E.26: Data (black) and synthetics (red), 6–30 s, from 9086693 to SWS.CI. Compare with Figure E.27.



1999 . 05 . 14
 9086693
 Mw = 3.90
 depth = 3.98 km
 SMTC . AZ
 dist = 132.0 km
 az = 156.5 deg
 --
 bp [6 s, 30 s]
 model m16

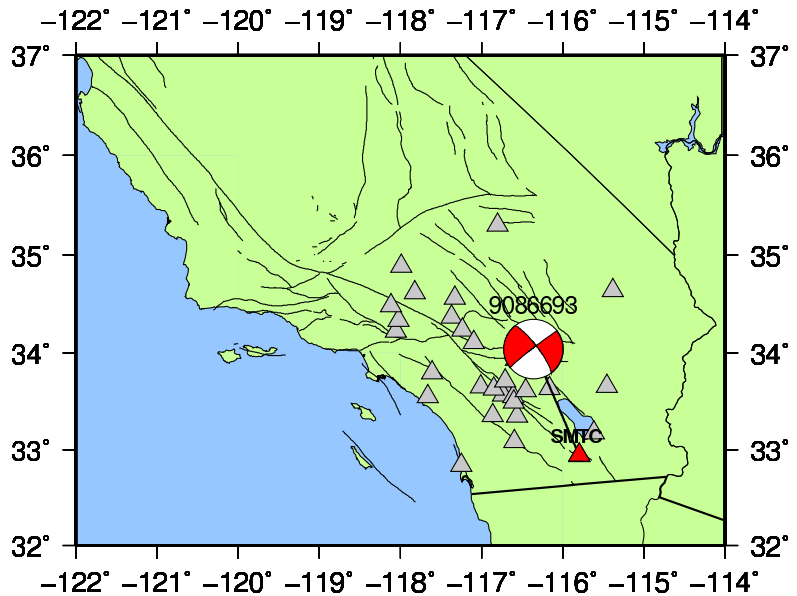
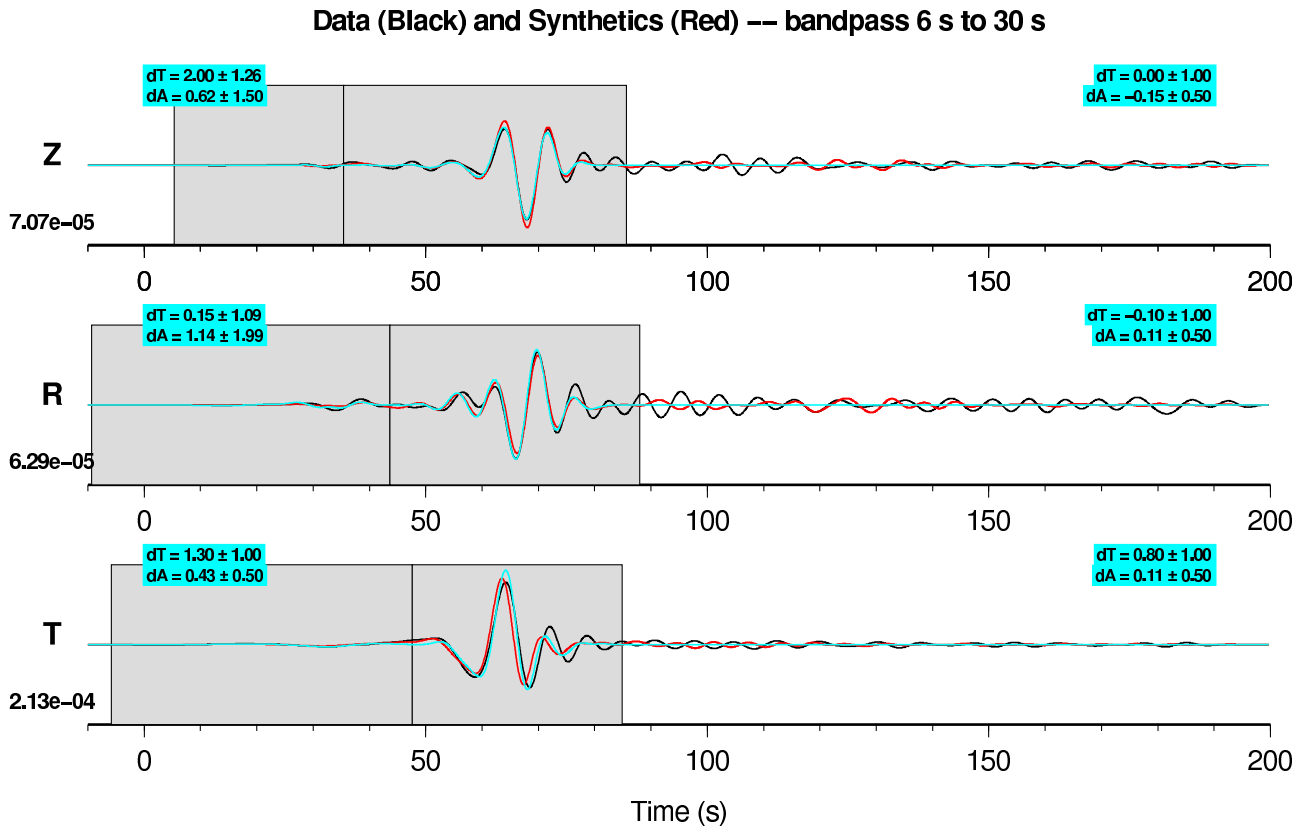


Figure E.27: Data (black) and synthetics (red), 6–30 s, from 9086693 to SMTC.AZ. The amplification problem is most apparent on the vertical and transverse components for this north-south path. Compare with Figure E.26.



1999 . 10 . 22
 9114812
 Mw = 4.85
 depth = 3.02 km
 JCS . CI
 dist = 197.8 km
 az = 185.1 deg
 --
 bp [6 s, 30 s]
 model m16

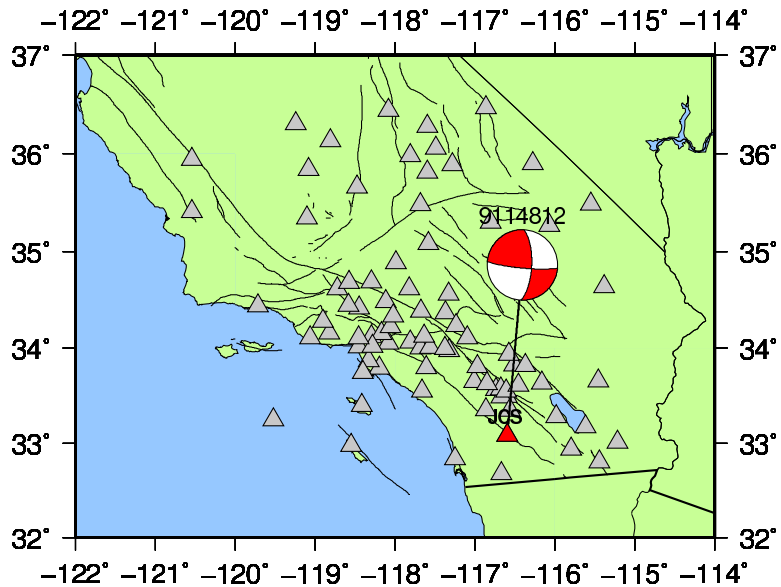


Figure E.28: Data (black) and synthetics (red), 6–30 s, from 9114812 to JCS.CI. Compare with Figure E.29.

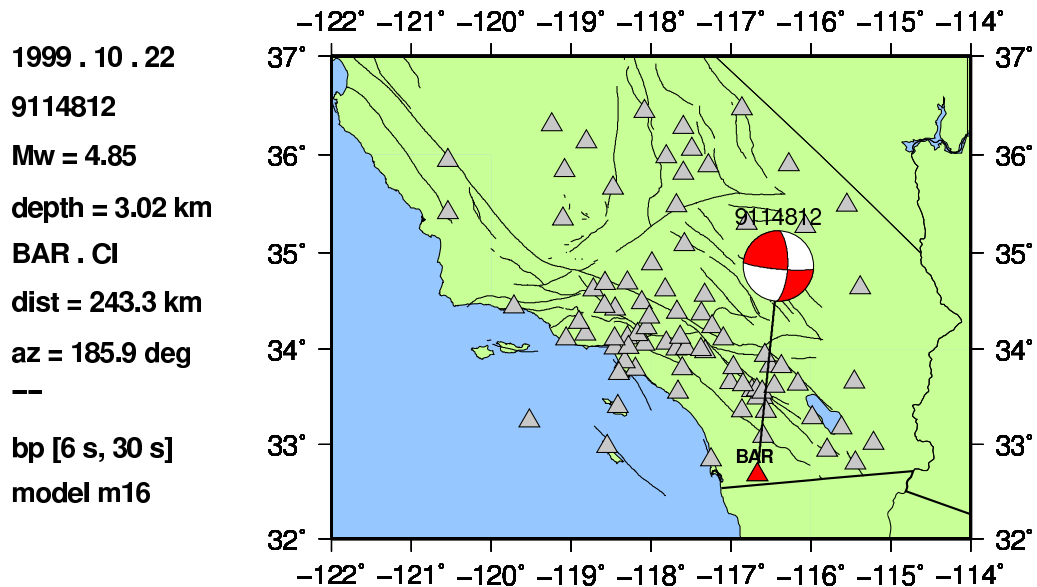
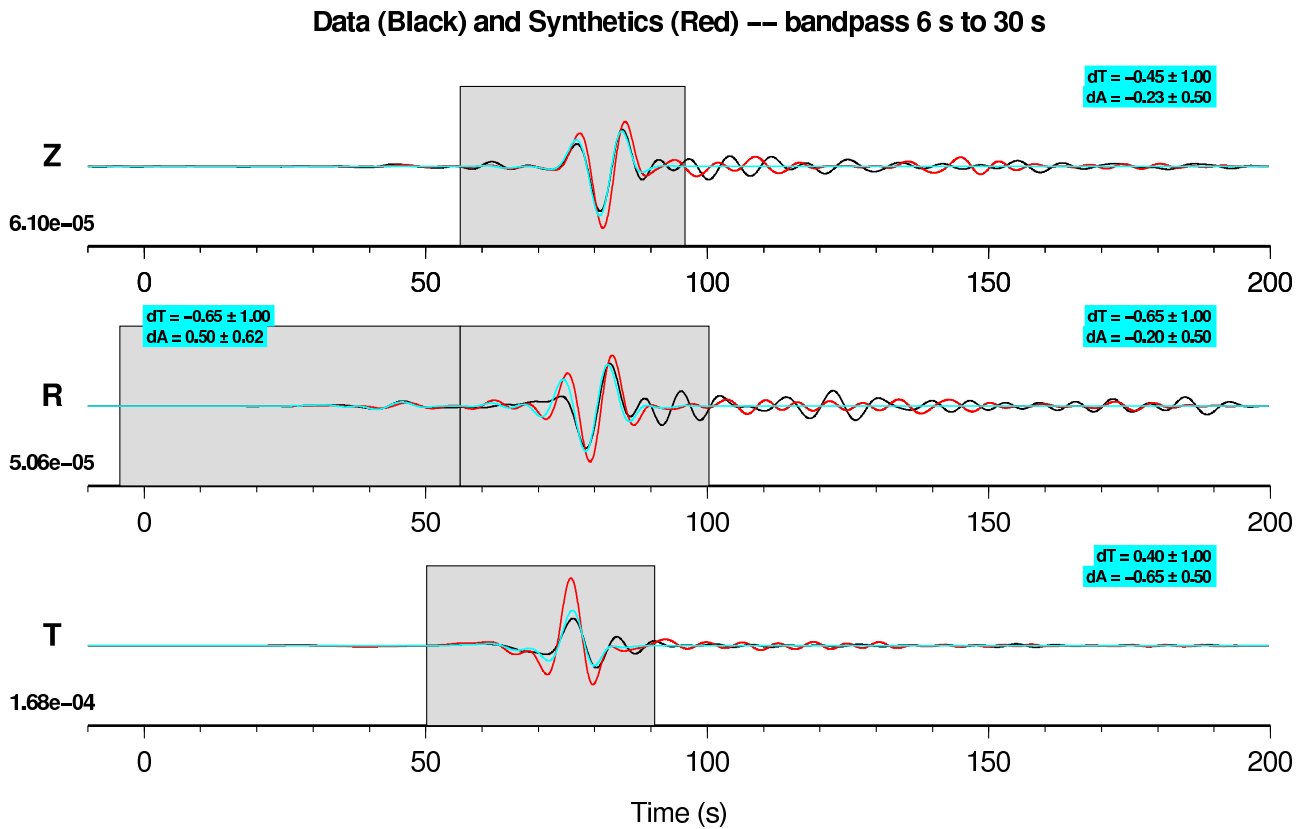


Figure E.29: Data (black) and synthetics (red), 6–30 s, from 9114812 to BAR.CI. Note that the amplification problem on this north-south-oriented path is only on the transverse component. Compare with Figure E.28.